PHYSICAL REVIEW B VOLUME 8, NUMBER 10 15 NOVEMBER 1973

Deep-Hole Excitations in Solids. II. Plasmons and Surface Effects in X-Ray Photoemission*†

Jhy-Jiun Chang‡ and David C. Langreth
Department of Physics, Rutgers, The State University, New Brunswick, New Jersey 08903
(Received 30 May 1973)

The theory of x-ray photoemission (and related experiments) involving the excitation of a core state interacting with plasmons is presented. Specifically, the effects of the solid surface have been calculated, thus complementing the authors' previous calculation of the bulk effects. The strengths of the surface- and bulk-plasmon satellites associated with (i) the sudden appearance of the deep hole, (ii) the escape of the photoelectron, and (iii) interference between these have been calculated.

I. INTRODUCTION

X-ray photoemission[1] as well as other forms of high-energy-electron spectroscopy have become widespread tools for the investigation of the electronic structures of materials. Such experiments however have always been difficult to interpret because of the presence of many-body and surface effects. In fact, the calculated[2] inelastic mean free path of a 1.5-keV electron is only about 15 Å and this has been recently confirmed by many experiments.[3] Thus, one might expect surface effects to play a role even at these energies. To study this problem we adopt a simple model[4,5] which contains plasmons as the most important many-body excitations at high energies. Such a model provides neither an extremely accurate description of the many-body effects, nor of the surface, but is expected not only to provide a good estimate of the magnitudes of the various effects involved, but also to serve as a prototype for more sophisticated calculations involving the accurate wave functions of the surface excitations when these become well known enough to make such a calculation worthwhile. The description which we give here is couched in the language of x-ray photoemission, although our calculation is easily adapted to other types of experiments involving the excitation or de-excitation of a core electron. The plasmon bulk effects in such experiments have been investigated in great detail in our previous work.[6] There we considered all the effects up to the order of $e^2/\hbar v$, where v is the velocity of the fast electron. The surface effects we consider here include the excitation of surface plasmons, the modification of the bulk-plasmon charge density, and the modification of the coupling between electron and plasmon.

Throughout this work we will be specifically discussing x-ray photoemission and will have in mind roughly the following situation: a 1.5-keV photon impinges on a solid, exciting a core electron which then escapes; it will always be assumed that the core electron was sufficiently tightly bound so as to be regarded occupying a single level, but not so deep as to have been lifetime broadened to a significant degree. It is also assumed that the escaping photoelectron is sufficiently energetic that its coupling constant $e^2/\hbar v \simeq (13.6\ \mathrm{eV}/E)^{1/2}$ can be treated as an expansion parameter. Even in this simplest situation, the various many-body effects are nontrivial and not small.

We will be interested in the various many-body effects which add structures to the basic photoemission line and the effects of the surface on these. One of these is the excitation of electron-hole pairs, which are responsible for the Mahan-Nozières-De Dominicis singularity[7,8] which has been discussed in the context of the photoemission problem by Doniach and Šunjić[9] and implicitly by Langreth.[10] They are also responsible, on the atomic level for the so called "shake-up" satellites discussed for example by Rosenwaig[11] *et al.* Finally, the excitation of multiple electron-hole pairs subtracts spectral weight from the main line and other sharp features, and displaces it to the background.[12] Since this paper deals principally with the effect of collective oscillations or plasmons, this latter electron-hole effect is the only one discussed. Essentially we will be calculating the weights of the various plasmon satellites to the x-ray photoemission line up to order $e^2/\hbar v$, although the methods developed are suitable for applications to some of the electron-hole effects as well.

Physically, the many-body effects arise in three different ways: (a) modification of the spectral density of the deep hole left behind when the photoelectron is excited; (b) inelastic scattering of the escaping photoelectron; and (c) interference between (a) and (b). We will also refer to (a) and (c) as *intrinsic* effects, while (b), the energy loss of the fast electron, will often be termed an *extrinsic* effect. In a previous work,[13] one of us has discussed these intrinsic many-body effects with respect to different types of experiments. The conclusion was that they tend to be "strong" (or rather of the order of the electron-gas coupling parameter $\sim r_s/6$) in experiments where the number of "slow" electrons is not conserved—for the purpose of this argument, nonrecoiling deep core elec-

trons as well as electrons near the Fermi level are considered "slow." On the other hand, if the number of "slow" electrons is conserved, then these intrinsic many-body effects are expected to be weak, as has long since been pointed out[14] in the cases of x-ray emission and absorption. Unfortunately, the extrinsic effects are invariably present in those experiments where the intrinsic effects are strong, and this makes their identification difficult. As discussed earlier, even though the coupling of the fast electron to the many-body excitations $e^2/\hbar v$ may be small, the extrinsic effects may not be small[6,13] because of the repeated nature of the interaction.

As pointed out for example by Hedin *et al.*,[15] the most important intrinsic effect in x-ray photoemission is the renormalization of the spectral density $A(\omega)$ of the deep hole, or item (a) above. Within the approximation (similar to that made in their paper) that the plasmon is an elementary excitation of the system, Langreth[5,10] has provided the exact solution for this spectral density and Hedin *et al.*[15] has made a numerical calculation of the spectrum using this solution. One prediction is that the strength of the nth plasmon satellite (due to this intrinsic effect above) is

$$e^{-\beta}\beta^n/n!, \tag{1a}$$

where

$$\beta=\sum_q \frac{g_q^2}{\omega_q^2} \tag{1b}$$

and

$$g_q^2=\left(\frac{4\pi e^2}{q^2}\right)\left[\frac{\partial\epsilon(q,\omega)}{\partial\omega}\bigg|_{\omega=\omega_q}\right]^{-1}, \tag{1c}$$

where ω_q is the plasmon frequency which occurs at the zero of the dielectric function $\epsilon(q,\omega)$. For a simple "metal" $\beta\simeq r_s/6$ where r_s is the radius of the Wigner-Seitz sphere in units of the Bohr radius; therefore $\beta\sim\frac{1}{3}$ for Al, Si, and Ge but can be considerably larger for the lower-density metals, notably the alkalis. What is done in Sec. III of this paper is to extend these results to the case where the deep hole is created near the surface, which is necessarily the case in a photoemission experiment. We find there that with the hole sufficiently close to the surface, the surface effect is quite large: First, some of the spectral weight is removed from the main peak and especially from the bulk-plasmon peaks and displaced to surface-plasmon peaks which now appear in the deep hole's spectral density. Second, the whole spectrum is shifted by an amount which can be as large as several electron volts for a deep hole very near the surface; deep inside an insulator this shift has a long range tail which has the classical image potential form $(e^2/4X)[(\epsilon-1)/\epsilon(\epsilon+1)]$. Our diagrammatic procedure calls for averaging the deep-hole spectral density in a manner which physically represents accounting for the escape probability. When this is done, the main peak, for example, takes on an asymmetric (but narrow) form but which in an incubator has a long tail, with the spectral density of those electrons arising near the surface being lost in the tail. These effects (after averaging) turn out to be fairly small for a photoelectron of 15-Å inelastic escape depth, and hence probably are not too significant unless the photoelectron's energy is down around several hundred eV, in which case the escape depth would be less than this.

The second intrinsic effect, labeled a "fast-slow" correction in Paper I[6] is the interference term between the photoelectron in the conduction band and the deep hole left behind. In the absence of a surface, this term was calculated in I to lowest order in $e^2/\hbar v$ which there as well as here is a small parameter. The calculation there may be taken over directly and applied to the photoemission experiment. The effect of the term is then to weaken any plasmon satellite by transferring spectral weight in the fractional amount $(e^2/\hbar v)F$ (where F is a slowly varying function of order unity) from a satellite to the next lower satellite (or to the main peak in the case of the first satellite). Since satellite strength from other sources tend to be monotonically decreasing, this interference term has the net effect of *weakening* the satellites from other sources. At high electron energies this weakening is relatively unimportant, but it becomes stronger as the electron's energy is lowered. It is shown in this paper, that the presence of the surface has no effect on this term, at least to the order of this calculation.

Finally there is the extrinsic effect which is simply the energy loss of the escaping electron. This is something which is common to a number of kinds of experiments and which an experimentalist usually wants to subtract out of his data, especially if he is measuring, for example, a valence-band structure; it is of course incorrect to assume that "line spectra" (as described in this paper) determines this directly, because the intrinsic effects are always present as well. In our previous paper, the extrinsic effects or fast-fast correction went under the heading of "admittance function." There it was calculated for a different experiment, but in the absence of any effects attributable directly to the presence of the surface, we may take over the results there, although "escape function"[16] would be a more reasonable name in a photoemission experiment. The fact that we are primarily interested here in calculating the strength of the various plasmon satellites makes possible a simplified point of view. This is because once the electron

excites an electron-hole pair on its way toward the surface its energy is smeared over a range of 20 eV or more, and is lost to the background so far as producing any sharp structures such as plasmon satellites is concerned.[15] If α is the probability that in a given interaction the escaping electron emits a plasmon rather than an electron-hole pair, then the strength of the nth satellite associated with this extrinsic effect was shown in I to be equal to α^n. The most important surface correction to this result is the rather trivial possibility that the escaping electron emits a surface plasmon; this gives a surface-plasmon satellite with strength of order $e^2/\hbar v$ in essential agreement with earlier calculations.[17] The other various effects, such as the deviation of the photoelectron self-energy from a local step function and the modification of the bulk plasmons charge density, combine to give a correction of the same orders as the fast-slow interference term mentioned earlier. Like the latter correction, this term further weakens the bulk-plasmon satellite.

In summary, then, surface effects are not very important at the higher electron energies ($\gtrsim$ keV) and are calculated quantitatively in our model as this energy is lowered. Neglecting these, the strength of the nth plasmon satellite (if the main line is normalized to unit strength) is equal to the coefficient of x^n in the expansion of

$$e^{\beta x}[(1-\alpha x)^{-1}], \tag{2}$$

where the exponential represents the intrinsic effect and the quantity in brackets is the extrinsic effect. The fast-slow interference term can be included in (2) simply as a velocity-dependent weakening of β [$\beta \to \beta - (e^2/\hbar v)F$], although as mentioned earlier, the surface produces a weakening of α of the same order of magnitude.

Aside from the theoretical interest in the intrinsic effect, it would be important to separate experimentally the extrinsic and intrinsic effects, because the extrinsic energy-loss effect occurs in other types of experiments too. Note that (2) predicts[18] that the strength of each successive satellite falls off faster than linearly (at least for $\beta < 1$) while the extrinsic effect alone would cause a linear falloff [that is, the strength of the $(n+1)$th satellite would be α times the strength of the nth]; this may provide a method for identifying the existence of the intrinsic effect.[19] One might also be able to see the velocity-dependent weakening effect by varying the energy of the incident x-rays. Finally the extrinsic (escape function) effect might be measured directly by another experiment: As shown in I, electron energy loss with core excitation in the back scattering geometry measures the same extrinsic effect (neglecting the surface) as photoemission, and in addition the intrinsic effects are expected to be quite small in the energy-loss experiment.[20]

II. MODEL AND DIAGRAMMATIC METHOD

We assume in our model that the solid occupies the whole space $x \leq 0$. For $x > 0$ we have vacuum. The surface is assumed smooth and not contaminated. Inside the solid we have uniformly distributed filled core state with binding energy Δ. The core states are assumed to be localized, that is, they have Δ-function-type wave functions. This is a reasonable approximation even for photon with energy as large as 5 keV. In this case the photon wavelength is about 2.5 Å, which is still much larger than the radius of the core electron.

Essentially we wish to calculate the dc current a long way outside the surface. For simplicity we assume that the measuring device has reasonable collimation and measures only those electrons escaping approximately normally to the surface; our method of course is easily generalized to an arbitrary angle, or average over angles. As long as for those angles the perpendicular velocity of the photoelectron $v_\perp \gg \omega_B/q_c$. This generalization is described in Appendix E. This perpendicular contribution to the photocurrent is expressible simply in terms of the one-particle correlation function

$$j(\vec{R}, t, p) = \int d^3r\,(-2ep)\,e^{i\vec{p}\cdot\vec{r}}\,\langle \psi^\dagger(\vec{R}+\tfrac{1}{2}\vec{r}, t)\psi(\vec{R}-\tfrac{1}{2}\vec{r}, t)\rangle$$

expanded to second order in the electromagnetic field representing the photon, as pointed out by Ashcroft and Schaich,[21] Mahan,[22] and others.[23] The systematics of a diagrammatic expansion for $G^<$ is standard.[24,25]

The basic process can be illustrated by Fig. 1. Since we do not have translational invariance in the x direction, we will work in real space instead of momentum space. Now we have photons with energy Ω incident normally[26] to the surface of the solid and excite a deep core electron at $\vec{X} = (X, \vec{X}_\parallel)$[27] with the x component of $\vec{X}$, $X < 0$. We record the escaping fast electron at $\vec{R} = (R, \vec{R}_\parallel = 0)$ far from the solid. The black squares are the matrix elements of the photon–core-electron interaction and have the form

$$M(\vec{X}) \sim M e^{X/26}\,\theta(-X),$$

where δ is the skin depth of the solid and $\theta(X)$ is the unit step function which vanishes for $X < 0$. We neglect the dependence of M on the energies of the escaping electrons. Since the escaped electrons to be interested in have energies much larger than the plasmon energy, this clearly is a good approximation.

With all this, Fig. 1 gives for $f(p, R; \Omega)$, the electron number density distribution function at point R with momentum p, the following expression:

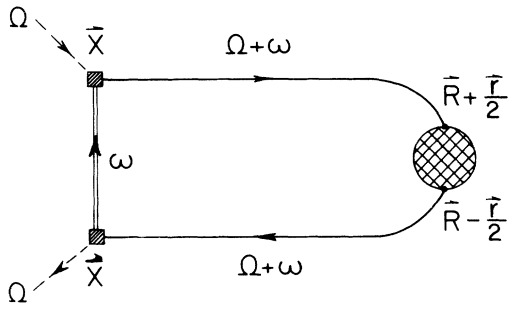

FIG. 1. Basic process for x-ray photoemission experiment involving the excitation of a deep core electron. The broken lines, the double line, and the single lines represent, respectively, the propagators for photons, deep core electron, and fast escaping electrons. The black dot is the response function of the measuring apparatus centered at $\vec{R}$. The black squares are the matrix elements for the photon–core-electron interaction.

$$f(p,R;\Omega)=|M|^2\int d^3r\int d^3X\, e^{X/\delta}\theta(-X)A_0(\omega,\vec{X})\times G(\vec{X},R+\tfrac{1}{2}\vec{r};\Omega+\omega+i\eta)\times G(R-\tfrac{1}{2}\vec{r},\vec{X};\Omega+\omega-i\eta)\,e^{i\vec{p}_\perp\cdot\vec{r}}, \quad (3a)$$

where Ω is the photon energy; $A_0(\omega,X)$ is the ensemble average of the deep-core-electron spectral density at X; while G's are fast-electron Green's functions to be defined later. We have let $\vec{p}=(p,\vec{p}_\parallel=0)$, because it is those electrons coming out of the solid approximately normal to the surface we are interested in and those electrons have only momentum in the x direction.

In real experimental situations, one measures the photocurrent instead of the number density distribution function $f(p,r,\Omega)$. The photocurrent contributed by the basic process is

$$j(p,r,\Omega)=-2epf(p,r,\Omega). \quad (3b)$$

The effect of the solid on the fast electron is partly taken care by an imaginary self-energy Σ_a which is assumed to be a local step function in real space;

$$\Sigma_a(\vec{x},\vec{x}';\omega\pm i\eta)=\mp i(1/2\tau)\,\delta(\vec{x}-\vec{x}')\theta(-x)\,. \quad (4)$$

The quantity $\tau\simeq[(e^2/\hbar v)\hbar\omega_p\ln(mv^2/\hbar\omega_p)]^{-1}$ is the lifetime[2] of the fast electron with velocity $v=2\sqrt{\omega}$.[28] In real cases, of course, the self-energy of the fast electron is neither a local nor a step function. Nevertheless, we will take this as a starting point and show later that the corrections are small ($\sim e^2/\hbar v$) by considering the lowest-order perturbation expansion of the difference between the true self-energy Σ_r and the approximate Σ_a.

The Green's functions of the fast electron are defined as

$$G(\vec{x},\vec{x}';\omega\pm i\eta)=\int\frac{d\omega}{2\pi}\,\frac{\tilde{A}(\vec{x},\vec{x}';\omega')}{\omega-\omega'\pm i\eta}\,, \quad (5)$$

where η is a infinitesimal positive number and $\tilde{A}(\vec{x},\vec{x}';\omega')$ is the spectral density of the fast electron with energy ω'. $G(x,x';\omega\pm i\eta)$ obeys the following equations:

$$[\omega\pm i\eta+\nabla^2+V(\vec{x})]G(\vec{x},\vec{x}';\omega\pm i\eta)=\delta(\vec{x}-\vec{x}')+\int d^3x''\,\Sigma_a(\vec{x},\vec{x}'';\omega\pm i\eta)G(\vec{x}'',\vec{x}';\omega\pm i\eta), \quad (6a)$$

$$[\omega\pm i\eta+\nabla^{2\prime}+V(\vec{x}')]G(\vec{x},\vec{x}';\omega\pm i\eta)=\delta(\vec{x}-\vec{x}')+\int d^3x''\,G(\vec{x},\vec{x}'';\omega\pm i\eta)\,\Sigma_a(\vec{x}'',\vec{x};\omega\pm i\eta), \quad (6b)$$

where $V(x)$ is the self-consistent potential of the solid. Since the mean free path is assumed to be much greater than the healing length of potential, we can take $V(x)$ to be a step function $V(x)=V\theta(x)$ for the purposes of this calculation. The magnitude of V, in general, is about 10 eV, which is much smaller than the energy of the photoelectron. It is evident that $G(x,x';\omega\pm i\eta)$ can be written as

$$G(\vec{x},\vec{x}';\omega\pm i\eta)=\sum_{\vec{k}_\parallel}e^{i\vec{k}_\parallel\cdot(\vec{x}-\vec{x}')}g(\vec{k}_\parallel;x,x';\omega\pm i\eta) \quad (7)$$

due to the translational invariance in the plane parallel to the surface. Upon substitution of (7) into Eq. (6), it can be shown that $g(\vec{k}_\parallel;x,x';E\pm i\eta)$ satisfies Eq. (6) with the first term replaced by $\omega-\vec{k}_\parallel^2$. These one-dimensional equations have been solved by Langreth[23] [Eq. (26) of that paper.] Since we are interested in the contribution to the current due to electrons escaping perpendicularly to the surface, the summation on $\vec{k}_\parallel$ is restricted to $|\vec{k}_\parallel|\sim 0$; The more general case is discussed in Appendix E. Therefore it is reasonable to neglect $\vec{k}_\parallel$ altogether. This is a good approximation even for electrons exciting several plasmons before they escape, because the plasmon wave vectors are restricted by the condition $|\vec{q}|\leq|\vec{q}_c|\ll|\vec{k}|$, where $\vec{k}$ is the momentum of the fast electron. Anyway, ignoring $\vec{k}_\parallel$ means neglecting a correction of order $|\vec{q}_c|^2/\omega\sim\omega_p^2/4\epsilon_f\omega\sim(e^2/\hbar v)^2$. Since we are interested in correction up to order $e^2/\hbar v$, this is a correction beyond our consideration.

By using Eqs. (3a) and (7) and the fact that owing to the symmetry of the model $A(\omega,\vec{X})$ does not depend on $\vec{X}_\parallel$, Eq. (3b) can be simplified as

$$j_0(P,R;\Omega)=-2ep|M|^2\int_{-\infty}^{+\infty}d\omega\int_{-\infty}^{+\infty}dr\,e^{ipr}\int d^3\vec{X}\times e^{X/\delta}\theta(-X)A(\omega,X)\times g(0;R-\tfrac{1}{2}r,X;\Omega+\omega+i\eta)\times g(0;X,R+\tfrac{1}{2}r;\Omega+\omega-i\eta). \quad (8)$$

From Eq. (2b) of II, we have

$$g(x,x';\omega+i\eta)=g(0;x',x;\omega-i\eta), \quad (9a)$$

$$g(x,x';\omega-i\eta)=\frac{i}{\sqrt{\omega}+(\omega-v)^{1/2}-i/2l}\times\exp\left[-i\sqrt{\omega}x+i\times\left((\omega-v)^{1/2}-\frac{i}{2l}\right)x'\right],\quad(9b)$$

where $l=v\tau$ is the mean free path of the fast photoelectron. Since $(1/2\sqrt{\omega})\,[\sqrt{\omega}-(\omega-v)^{1/2}]\sim v/4\omega \sim (1\text{ Ry})/\omega$ and $1/(\omega l^2)^{1/2}\sim(e^2/\hbar v)\,(\hbar\omega_p/\omega)\ln(2\omega/\hbar\omega_p)\ll e^2/\hbar v$, while $e^2/\hbar v\sim[(1\text{ Ry})/\omega]^{1/2}$, Eq. (9b) can be simplified to give

$$g(x,x';\omega-i\eta)\simeq\frac{i}{2\sqrt{\omega}}\times\exp\left(-i\sqrt{\omega}\,(x'-x)-i\frac{v}{2\sqrt{\omega}}x'+\frac{x'}{2l}\right),\qquad x>0,\quad x'<0.\quad(10a)$$

The other components of the partial fast-electron Green's function $g(x,x',\omega)$ can be written down without further approximation as

$$g(x,x';\ \omega-i\eta)\simeq\frac{i}{2\sqrt{\omega}}\times\exp\left[i\left(\sqrt{\omega}-\frac{i}{2l}\right)x-i\left(\sqrt{\omega}-\frac{v}{2\sqrt{\omega}}\right)x'\right],\qquad x<0,\quad x'>0\quad(10b)$$

$$g(x,x';\ \omega-i\eta)\simeq\frac{i}{2\sqrt{\omega}}\exp\left[-i\left(\sqrt{\omega}-\frac{v}{2\sqrt{\omega}}\right)(x-x')\right],\qquad x>0,\quad x'>0\quad(10c)$$

$$g(x,x';\ \omega-i\eta)\simeq\frac{i}{2\sqrt{\omega}}\exp\left[-i\left(\sqrt{\omega}-\frac{i}{2l}\right)|x-x'|\right],\qquad x<0,\quad x'<0.\quad(10d)$$

Now, with the approximate Green's function, Eq. (8) becomes

$$j_0(P,R,\Omega)=-2ep|M|^2\int_{-\infty}^{0}dX\int_{-\infty}^{+\infty}d\omega\,\frac{e^{X(1/\delta+1/l)}}{4(\Omega+\omega)}\times A(\omega,X)\,\delta(P-(\Omega+\omega-v))^{1/2}.\quad(11)$$

From now on we set $\delta=0$, since $\delta\gg l$, the inelastic escape depth of the fast electron which has energy ~keV.

For the electron-plasmon interaction, we take our model Hamiltonian to be[4,5]

$$H_{e\text{-}pl}=\sum_{\vec{q}}g_{qB}\,\psi^{\dagger}(\vec{x})\psi(\vec{x})\,a_{\vec{q}}\sin q_{\perp}x\,e^{i\vec{q}\cdot\vec{x}_{\parallel}}\theta(-x)+\sum_{\vec{q}_{\parallel}}g_{qS}\,\psi^{\dagger}(\vec{x})\,\psi(\vec{x})\,b_{\vec{q}_{\parallel}}\exp(i\vec{q}_{\parallel}\cdot\vec{x}_{\parallel}-|\vec{q}_{\parallel}||x|)+\text{c.c.},\quad(12)$$

where $a_{\vec{q}}$ and $b_{\vec{q}}$ are destruction operators for bulk (B) and surface (S) plasmons, respectively, while $\psi^{\dagger}(\vec{x})$ and $\psi(\vec{x})$ are electron field operators. Summation $\vec{q}$ is restricted to $|\vec{q}|<q_c$. Also, we have q, the x component of the wave vector $\vec{q}$ be positive. The surface-plasmon wave vectors $\vec{q}_{\parallel}$ have only the component parallel to the surface survive. The matrix elements for electron-plasmon interaction g_{qB} and g_{qS} are taken to be

$$g_{qB}=\left(2\frac{4\pi e^2}{q^2}\frac{1}{\partial\epsilon(q,\omega)/\partial\omega}\bigg|_{\omega_q}\right)^{1/2};\qquad g_{qS}=\left(\frac{4\pi e^2}{|\vec{q}_{\parallel}|}\frac{1}{\partial\epsilon(q,\omega)/\partial\omega}\bigg|_{\omega_{sq}}\right)^{1/2},\quad(13)$$

where ω_q and ω_{sq} are bulk- and surface-plasmon frequencies which satisfy the conditions

$$\epsilon(q,\omega_q)=0;\quad\epsilon(q,\omega_{sq})=-1\quad(14)$$

choosing the dielectric function to be of the form

$$\epsilon(q,\omega)=1-\omega_p^2/(\omega^2-\Delta_q^2)\quad(15)$$

will suffice for our purposes, where $\Delta_q\propto q$ for metals for small q and, for insulators $\Delta_q\sim$ constant which is about the gap energy between conduction and valence bands. This dielectric function gives correct values at $\omega\to 0,\ \infty$ limits. Upon the substitution of Eq. (15) in (13) and neglecting the dispersions of the plasmon frequencies the matrix elements g_{qB} and g_{qS} become

$$g_{qB}=\left[\frac{4\pi e^2}{q^2}\hbar\omega_B\left(1-\frac{1}{\epsilon}\right)\right]^{1/2};\qquad g_{qS}=\left[\frac{\pi e^2}{|\vec{q}_{\parallel}|}\hbar\omega_S\left(\frac{\epsilon-1}{\epsilon-1}\right)\right]^{1/2},\quad(16)$$

where ϵ is the static dielectric constant of the solid and

$$\omega_B=\omega_p\left(1-\frac{1}{\epsilon}\right)^{-1/2};\quad\omega_S=\frac{\omega_p}{\sqrt{2}}\left(\frac{\epsilon-1}{\epsilon+1}\right)^{-1/2}\quad(17)$$

are, respectively, the bulk and surface frequencies without dispersion. For metals, $\epsilon\to\infty$, $\omega_B=\omega_p$, and $\omega_S=\omega_p/\sqrt{2}$, Eq. (16) reduces to the coupling constants obtained by Gersten[4] and others.[15]

III. SPECTRAL DENSITY OF THE DEEP HOLE

When we turn on the electron-plasmon interaction $H_{e\text{-}pl}$ [Eq. (12)], aside from the modification of the fast electron's mean free path which has been partly taken care of by using an approximate self-energy Σ_a [Eq. (4)], we have plasmon effects associated with the three sources mentioned in Sec. I. The typical processes for each are shown in Fig. 2. We investigate here the plasmon effects associated with the modification of the deep-hole spectral density, i.e., we use the renormalized deep-hole sprectral density instead of the bare one in Fig. 1. The renormalized deep-hole Green's function $G_h(t,\vec{X})$ is shown in Fig. 3. The

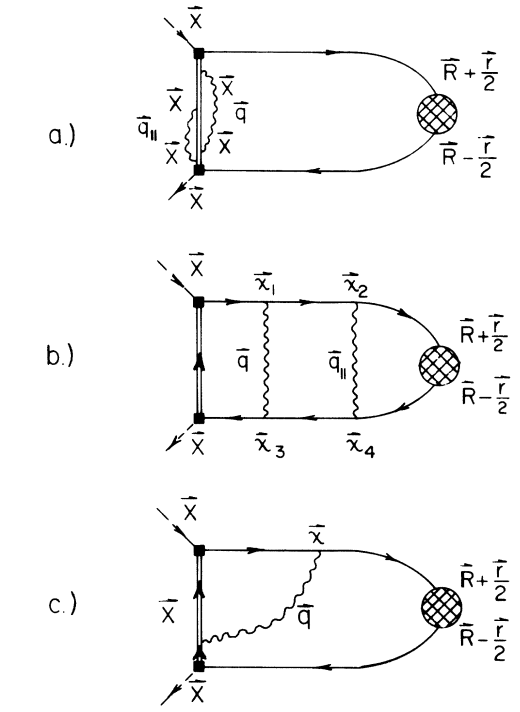

FIG. 2. Typical diagrams for plasmon effects associated with three sources: (a) typical renormalization of the deep-hole spectral density; (b) energy loss of the escaping photoelectron by the emission of two plasmons; (c) fast-slow interference or vortex correction. Here and elsewhere the wavy lines are plasmon propagators.

wavy line usually represents the effective Coulomb interaction $(4\pi e^2/q^2)^2 S(\vec{q}, \omega)$, $S(\vec{q}, \omega)$ is the dynamic structure factor, but in our approximation it is the plasmon propagator $D(\vec{q}, \omega)$ times the corresponding coupling constant g_q^2. We have in our model

$$D(\vec{q}, \omega) = 2\pi\delta(\omega - \omega_B), \tag{18}$$

and, owing to the local approximation of the deep hole, the ensemble average of the bare deep-hole Green's function is given by

$$g_h(t, \vec{X}) = ie^{i\Delta t}\,\theta(-X)\,\theta(-t). \tag{19}$$

By using the linked cluster theorem, $G_h(t, \vec{X})$ can be written down immediately as

$$G_h(t, \vec{X}) = ie^{i\Delta t}\exp\Big(-\sum_{\vec{q}} g_{qB}^2 \int_t^0 d\tau' \int_{\tau'}^0 d\tau \times e^{i\omega_B(\tau'-\tau)}\sin^2 q_\perp X - \sum_{\vec{q}_\parallel} g_{qS}^2 \int_t^0 d\tau' \int_{\tau'}^0 d\tau \times \exp[i\omega_S(\tau'-\tau) + 2|\vec{q}_\parallel|X]\,\theta(-X)\,\theta(-t)\Big). \tag{20}$$

Therefore the spectral density of the deep hole $A(\omega, X)$ is given by

$$A(\omega, X) = \frac{1}{\pi}\,\mathrm{Im}\int_{-\infty}^{\infty} dt\, e^{i\omega t} G_h(t, X) = \sum_{nm} A_{m,n}(\omega, X)$$
$$= e^{K(X)} \sum_{n,m=0}^{\infty} \frac{\beta_B^n(X)}{n!}\,\frac{\beta_S^m(X)}{m!} \times \delta(\omega + \Delta + n\omega_B + m\omega_S + \Delta E(X)), \tag{21}$$

where

$$\beta_B(X) = \sum_{\vec{q}} \frac{g_{qB}^2}{\omega_B^2}\sin^2 q_\perp X\,\theta(-X),$$
$$\beta_S(X) = \sum_{\vec{q}_\parallel} \frac{g_{qS}^2}{\omega_S^2} e^{2|\vec{q}_\parallel|X}\theta(-X), \tag{22}$$
$$-K(X) = \beta_B(X) + \beta_S(X), \quad -\Delta E(X) = \beta_B(X)\omega_B + \beta_S(X)\omega_S.$$

We discuss the energy shift $\Delta E(X)$ first and come back to consider the effect of $K(X)$ later. The energy shift can be separated into two parts. One, which we call $\Delta E_B (= -\beta_B\omega_B)$, is contributed by the bulk plasmon and the other, which we call ΔE_S $(= -\beta_S\omega_S)$ is contributed by the surface plasmon. A straightforward calculation gives

$$\Delta E_B(X) = -\beta\omega_B\Big(1 - \frac{1}{2q_cX}\,\mathrm{Si}(2q_cX)\Big) \sim \begin{cases} O(X^2) & \text{if } |X| \ll q_c^{-1} \\ -\beta\omega_B\Big(1 + \dfrac{\pi}{4q_cX}\Big) + O\Big(\dfrac{1}{X^2}\Big) & \text{if } |X| \gg q_c^{-1} \end{cases} \tag{23a}$$

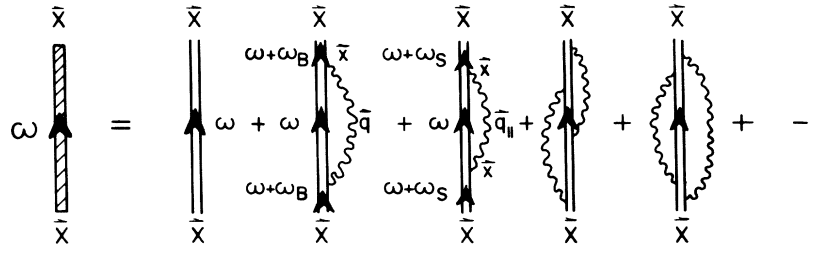

FIG. 3. Diagrammatic expansion of the real deep-hole Green's function in terms of the bare Green's function. $\vec{X}$ is where the deep hole is excited.

and

$$\Delta E_S(X) = \frac{e^2}{4X}\left(\frac{\epsilon-1}{\epsilon+1}\right)(1-e^{2q_cX}) \sim \begin{cases} \frac{e^2 q_c}{2}\left(\frac{\epsilon-1}{\epsilon+1}\right) - \frac{e^2 q_c^2 X}{2}\left(\frac{\epsilon-1}{\epsilon+1}\right) & \text{if } |X| \ll q_c^{-1} \\ \frac{e^2}{4X}\left(\frac{\epsilon-1}{\epsilon+1}\right) & \text{if } |X| \gg q_c^{-1}, \end{cases} \tag{23b}$$

where

$$\mathrm{Si}(X) \equiv \int_0^X \frac{\sin y}{y}\,dy \quad \text{and} \quad \beta = \frac{e^2 q_c}{\pi\omega_B}\left(1-\frac{1}{\epsilon}\right). \tag{24}$$

The very small oscillation in $\Delta E_B(X)$ contributed by $\mathrm{Si}(X)$ is due to the artificial cut-off plasmon wave vector q_c, and hence is unphysical. Adding (23a) and (23b) up, we obtain the total energy shift for the two limiting cases

$$\Delta E(X) = -\frac{e^2 q_c}{\pi}\left(1-\frac{1}{\epsilon}\right) - \frac{e^2}{4X}\frac{1}{\epsilon}\left(\frac{\epsilon-1}{\epsilon+1}\right) \text{ if } |X| \gg q_c^{-1}$$
$$= -\frac{e^2 q_c}{2}\left(\frac{\epsilon-1}{\epsilon+1}\right) \text{ if } |X| \ll q_c^{-1}. \tag{25}$$

$\Delta E(X)$, as well as ΔE_B and ΔE_S, is plotted in Fig. 4 by taking $\epsilon = 2, 5$. We point out here that when the core hole is far from the surface, i.e., for $|X| \gg q_c^{-1}$, both bulk and surface plasmons give energy shifts with the form of the image charge potential. For metals, $\epsilon \to \infty$ and the image charge potentials due to these two sources cancel completely. However, for insulators this cancellation is not complete. But, because of the factor $(1/\epsilon)[(\epsilon-1)/(\epsilon+1)]$, the image charge potential energy is small. Also worth noting is that $\beta_B(X)$ vanishes at the surface but restores its bulk value β [Eq. (2)] as $X \to -\infty$, while $\beta_S(X)$ has its maximum value at the surface and becomes smaller and smaller as $X \to -\infty$. The situations for $\Delta E_B(X)$ and $\Delta E_S(X)$ are similar to that of $\beta_B(X)$ and $\beta_S(X)$. From Fig. 4, it is clear that the broadening of the spectral line can be described *roughly* by the quantity

$$\Delta E(0^-) - \Delta E(-\infty) = \frac{e^2 q_c}{\pi}\left[\left(1-\frac{1}{\epsilon}\right) - \frac{\pi}{2}\frac{\epsilon-1}{\epsilon+1}\right], \tag{26}$$

which is the difference of the deep-hole energy shifts at the surface and that deep inside the sample. This quantity is smaller than the plasmon energy; therefore, this surface effect will not have the plasmon satellites overlapped. For example, for metal $\epsilon \to \infty$ and $q_c \sim \omega_p/v_f$, the difference of the shifts is about $(1-\frac{1}{2}\pi) r_s \hbar\omega_p/3\pi$ which is 4~5 eV at most.

Now we consider the modification of main peak strength owing to the surface effects on the deep-hole spectral density. It is obvious that so far the strength of the peak is concerned we can neglect the space dependence of the energy shift $\Delta E(X)$ because what it does is to redistribute the spectral weight within the peak (we show this explicitly in Appendix B). So, we use $A_{00}(\omega, X)$ for the deep-hole spectral density, where $A_{00}(\omega, X)$ is the term in $A(\omega, X)$ [Eq. (21)] with $n = 0$ and $m = 0$, i.e.,

$$A_{00}(\omega, X) = e^{K(X)}\delta(\omega + \Delta - \beta\omega_B)\theta(-X),$$
$$K(X) = \beta + \delta K(X),$$
$$\delta K(X) = \frac{e^2}{4X}\left[\frac{2}{\pi\omega_B}\left(1-\frac{1}{\epsilon}\right)\mathrm{Si}(2q_cX) + \frac{1}{\omega_S}\left(\frac{\epsilon-1}{\epsilon+1}\right)(1-e^{2q_cX})\right], \tag{27}$$

where $\delta K(X)$ is the correction due to the presence of solid surface. Although quite large close to the surface, $\delta K(X)$ has small effect on the photoemission spectrum. This is because $\delta K(X)$ is characterized by a distance q_c^{-1}. For $|X| \gg q_c^{-1}$, $\delta K(X) \sim 0$. While the inelastic escape depth of the photoelectron l is as small as 15 Å for a 15-keV electron, it is still much larger than q_c^{-1}. Therefore, we expect the leading term of correction due to $\delta K(X)$ to be of order $(lq_c)^{-1} \sim (e^2/\hbar v) \times (\omega_B/vq_c)\ln(mv^2/\omega_B)$, and hence it can be neglected. The reader will find the detailed calculation in Appendix B.

Aside from affecting the strength of the peaks, $\delta K(X)$ and $\Delta E(X)$ change the shape of the peaks also. For example, to see the line shape of the main peak we use $A_{00}(\omega, X)$ for the deep-hole spectral density; we substitute it into Eq. (11) and obtain $j_0(P, R, \Omega)$, the current density detected at R from those electrons without exciting a plasmon on their

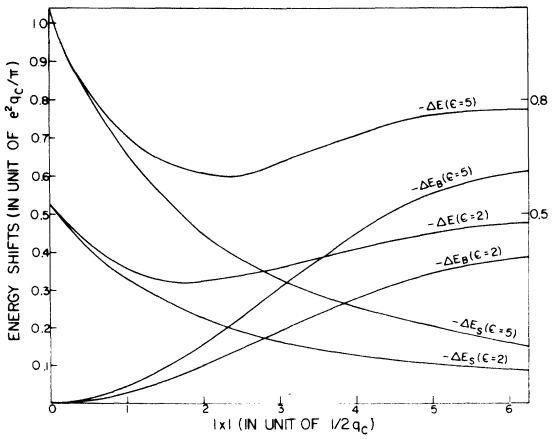

FIG. 4. Energy shifts of the deep core state due to bulk plasmon (ΔE_B), due to surface plasmon (ΔE_S), and their sum (ΔE) are plotted as function of distance from the surface by taking the static dielectric constant $\epsilon = 2, 5$.

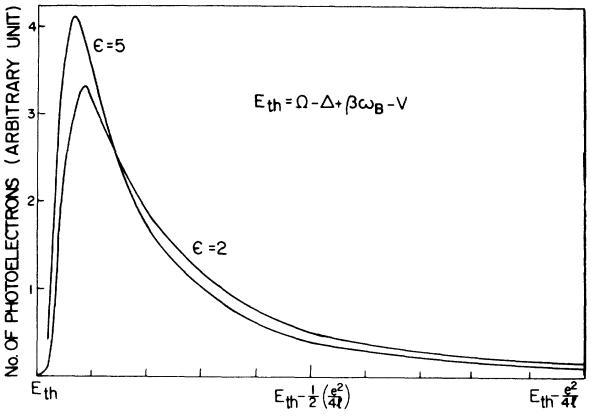

FIG. 5. Line shape of the main peak plotted in units of $e^2/4l$ (which is about $\frac{1}{4}$ eV for a 1.5-keV electron) for material with static dielectric constants $\epsilon = 2, 5$.

way out. $j_0(R, \Omega)$ is plotted in Fig. 5 for $\epsilon = 2, 5$. If there were no surface, the total weight would pile up at $E_{Th} = \Omega - \Delta + \beta\omega_B$. With the presence of the surface, the peak of the main satellite will shift to *lower* energy by an amount $\sim (e^2/4l)(1/\epsilon) \times [(\epsilon - 1)/(\epsilon + 1)]$ which for $l \sim 15$ Å, $\epsilon = 5$, is about $\frac{1}{15}$ eV $\ll 1$ eV. Also, we notice that the line shape of the main peak is asymmetric, there is a long tail, and it is those electrons originating close to the surface get lost in the tail. Essentially, the spectral line becomes flat when $E_{Th} - E \geq e^2/4l$, which for a 15-keV electron is about $\frac{1}{4}$ eV only. We find the fractional weight of the main peak falling outside this point is given by

$$1 - \exp\{-(1/\epsilon)[(\epsilon - 1)/(\epsilon + 1)]\}. \tag{28}$$

Taking $\epsilon = 5$, this is about 13%. Therefore the weight which gets lost in the tail is more than 13% and even larger if we consider electron escaped with a finite angle to the normal of the surface. But, in real experimental situations, because the resolution of the linewidth is larger (usually the resolution is ≥ 1 eV) than $e^2/4l \sim 1/4$ eV, the asymmetry of the peak and the loss of the weight may not be as significant as we calculated here.

Before we turn to the extrinsic effects and interference corrections we consider the first surface-plasmon satellite due to the normalization of the deep-hole spectral density. Since the electrons which contribute to the satellite do not excite any bulk plasmons, they originate, in average, at a distance l deeper inside the surface; while the surface-plasmon charge density decays exponentially away from the surface, we expect the surface-plasmon satellite due to this effect to be small. In fact, the strength ratio of this and the main peak is given by the expression

$$\frac{e^2}{4l}\,\frac{1}{\hbar\omega_S}\ln|q_c l| \sim \frac{1}{4}\left(\frac{e^2}{\hbar v}\right)^2\frac{\hbar\omega_B}{\hbar\omega_S}\ln\left(\frac{mv^2}{\hbar\omega_B}\right)\ln\left(\frac{vq_c}{\hbar\omega_B}\,\frac{\hbar v}{e^2}\right). \tag{29}$$

The detailed calculation is given in Appendix C. It is obvious that the correction to the bulk-plasmon satellite due to the modification of the deep-hole spectral density will be the same order as (29), and we will not consider it.

IV. EXTRINSIC EFFECTS: FAST ELECTRON-PLASMON CORRECTIONS

Before we consider any extrinsic effects, let us calculate the main peak whose strength is given incorrectly by Eq. (B3) in Appendix B because we used the approximate $\Sigma_a(\vec{x}, \vec{x}'; \omega \pm i\eta)$ [Eq. (4)] for the self-energy of the fast electron. The lowest-order corrections are shown in Fig. 6. The wavy lines in diagrams 6(a) and 6(b) are surface- and bulk-plasmon propagators, respectively, while the circle in diagram 6(c) represents the negative of the approximate self-energy $\Sigma_a(\vec{r}, \vec{r}'; \omega)$. Therefore, diagrams 6(b) and 6(c) together give the correction to the strength of the main peak due to the consideration of the real part and the nonlocal part of the fast-electron self-energy contributed by the bulk plasmon, and diagram 6(a) takes care of that by the surface plasmon. Of course there should be corrections due to the electron-hole pair excitations; however, we expect them to be small and shall not consider them here.

The contributions of diagram 6(a) and its complex conjugate to the strength of the main peak are given by the expression

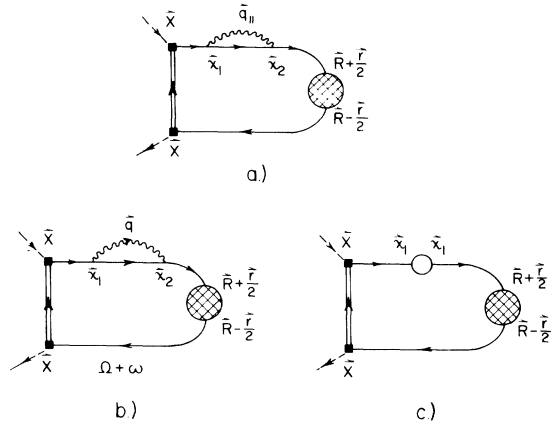

FIG. 6. Typical diagrams contributing to the lowest-order correction to the strength of the main peak by considering the real and nonlocal part of the fast-electron self-energy: (a) Correction to the self-energy due to surface plasmons; (b) is the bulk-plasmon self-energy correction, part of which has already been included by using a Green's function with a local imaginary self-energy; this double counted part is subtracted off by (c) where the circle represents the approximate self-energy Σ_a [Eq. (4)].

$$\Delta j_{0S}(p,R,\Omega)\simeq -2e|M|^2\int d\omega\int d^3\vec{r}\,pe^{i\vec{p}_\perp\cdot\vec{r}}\int d^3\vec{X}\,\theta(-X)\int d^3\vec{x}_1\int d^3\vec{x}_2\sum_{\vec{q}_\parallel}g_{qS}^2\exp[i\vec{q}_\parallel\cdot(\vec{x}_1-\vec{x}_2)-|\vec{q}_\parallel||x_1|$$
$$-|\vec{q}_\parallel||x_2|]A_{00}(\omega,X)G(\vec{X},\vec{x}_1;\Omega+\omega+i\eta)G(\vec{x}_1,\vec{x}_2;\Omega+\omega-\omega_s+i\eta)\,\theta(x_2-x_1)G(R-\tfrac{1}{2}\vec{r},\vec{X};\Omega+\omega-i\eta)$$
$$\times G(\vec{x}_2,R+\tfrac{1}{2}\vec{r};\Omega+\omega+i\eta)\theta(x_1-X)+\text{c.c.} \tag{30}$$

There are other terms corresponding to cases of ordering X, x_1, and x_2 differently. Since the escaped electrons are assumed to have high energy (~1 keV), these terms are small. Upon the substitution of the fast-electron Green's functions from Eqs. (7) and (10), we integrate over $\vec{r}$ and all the parallel components of $\vec{X}$, $\vec{x}_1$, and $\vec{x}_2$, and obtain the expression for $\Delta j_{0S}(P,R,\Omega)$. We have

$$\Delta j_{0S}(P,R;\Omega)\simeq 2ep|M|^2\int d\omega\int dX\,\theta(-X)\int dx_1\int dx_2\,\theta(x_2-x_1)\,\theta(x_1-X)$$
$$\times e^{X/l}A_{00}(\omega,X)\exp\left(-i\,\frac{\omega_S}{(\Omega+\omega)^{1/2}}(x_1-x_2)\right)\sum_{\vec{q}_\parallel}g_{qS}^2\exp(-|q_\parallel||x_1|-|q_\parallel||x_2|)$$
$$\times\frac{\delta(P-(\Omega+\omega-v)^{1/2})}{16(\Omega+\omega)^2}+\text{c.c.} \tag{31}$$

In the denominator we have made the approximation $\Omega+\omega-\omega_S\sim\Omega+\omega$. Also, in the phase factors we have taken $(\Omega+\omega-v-\omega_S)^{1/2}\sim(\Omega+\omega)^{1/2}-(V+\omega_s)/2(\Omega+\omega)^{1/2}$. These approximations together with the ignoring of $|\vec{q}_\parallel|^2$ in the fast-electron Green's function are equivalent to that of taking a classical path for the fast electron as Šunjić and Lucas[29] did with the problem of the energy loss for a fast electron passing through a thin film. The error involved represents a small correction to a small correction. Since we are interested in the strength of the main peak, we use $A_0(\omega)=e^{-\beta}\delta(\omega-\Delta+\beta\omega_B)$ for $A_{00}(\omega,X)$. By using this bulk deep-hole spectral density, we have neglected the effect of $\delta K(X)$ which is a correction to β in the exponent, but it has small effect on the strength of the satellites due to the considerations in Sec. III. Working out the rest of the integrations, we simplify Eq. (31), which becomes

$$\Delta j_{0S}(P,R;\Omega)=-\frac{B\delta(P-(\Omega-\Delta+\beta\omega_B-v)^{1/2})}{4(\Omega-\Delta+\beta\omega_B)}$$
$$\times\sum_{\vec{q}_\parallel}g_{qS}^2\left(\frac{4q_\parallel^2}{q_\parallel^2+(\omega_S/v)^2}+\frac{1}{q_\parallel^2+(\omega_S/v)^2}\,\frac{1}{(2q_\parallel+l^{-1})}-\frac{4q_\parallel^2(q_\parallel+l^{-1})+4q_\parallel(\omega_S/v)^2}{[q_\parallel^2+(\omega_S/v)^2][(\omega_S/v)^2+(q_\parallel+l^{-1})^2]}\right) \tag{32}$$

with $B\equiv -e|M|^2e^{-\beta}l/v$ defined by Eq. (B3), where $v=2(\Omega-\Delta-V+\beta\omega_B)^{1/2}$ is the velocity of the fast electron. The most important contributions come from the first term in the large parentheses which gives

$$\Delta j_{0S}(P,R;\Omega)=B\delta(P-(\Omega+\beta\omega_B-\Delta-V)^{1/2})\left[\frac{\pi}{2}\,\frac{e^2}{\hbar v}\left(\frac{\epsilon-1}{\epsilon+1}\right)\left(1-\frac{2}{\pi}\tan^{-1}\theta_S-\frac{2}{\pi}\,\frac{\theta_S}{1+\theta_S^2}\right)\right] \tag{33}$$

with $\theta_S=\omega_S/vq_c$. All other terms have contributions of order $(e^2/\hbar v)^2$ or higher. Therefore the modification of the fast-electron self-energy due to the surface plamson will reduce the strength of the main peak by a fraction of order $e^2/\hbar v$.

Now, we turn to calculate diagram 6(b). Its contribution to the strength of the main peak is given by the expression

$$j_{0(b)}(P,R;\Omega)=-2ep|M|^2\int d\omega\int d^3\vec{r}\,e^{i\vec{p}_\perp\cdot\vec{r}}\int d^3\vec{X}\,\theta(-X)\int d^3x_1\int d^3x_2\sum_{\vec{q}}g_{qS}^2e^{i\vec{q}_\parallel\cdot(\vec{x}_1-\vec{x}_2)}\sin q_\perp x_1\sin q_\perp x_2$$
$$\times A_{00}(\omega,X)\theta(-x_1)\theta(-x_2)G(\vec{X},\vec{x}_1;\Omega+\omega+i\eta)G(\vec{x}_1,\vec{x}_2;\Omega+\omega-\omega_B-i\eta)\theta(x_2-x_1)\theta(x_1-x)+\text{c.c.} \tag{34}$$

This equation is similar to Eq. (31) except for three points: First, the coupling constants are different. Second, we have the excitation energy ω_B instead of ω_S. Third, the bulk-plasmon excitations are restricted within the solid, whereas the excitations of the surface plasmon are symmetric with respect to the surface. Following the same method of calculating diagram 6(a) and without making any further approximation, we find

$$j_{0(b)}(P,R;\Omega) = -\tfrac{1}{8} B\delta(P-(\Omega-\Delta+\beta\omega_B-v)^{1/2}) \sum_{\vec{q}} g_{qB}^2 \left[\frac{1}{(\omega_B/v+q_\perp)^2+(l)^{-2}} + \frac{1}{(\omega_B/v-q_\perp)^2+l^{-2}} - \frac{1}{(\omega_B/v)^2-q_\perp^2} \right.$$
$$\left. \times \left(1 - \frac{1}{l^2}\frac{1}{(\omega_B/v+q_\perp)^2(l)^{-2}} - \frac{1}{l^2}\frac{1}{(\omega_B/v-q_\perp)^2+l^{-2}} + \frac{1}{l^2}\frac{1}{4q_\perp^2+l^{-2}}\right)\right] . \quad (35)$$

After summing over $\vec{q}$, Eq. (35) can be simplified further as

$$j_{0(b)}(P,R,\Omega) = B\delta(P-(\Omega-\Delta+\beta\omega_B-v)^{1/2})\left[-\alpha - \frac{1}{\pi}\frac{e^2}{\hbar v}\left(1-\frac{1}{\epsilon}\right)\ln\left|\frac{1+\theta}{1-\theta}\right| + \frac{1}{2}\frac{e^2}{\hbar v}\left(1-\frac{1}{\epsilon}\right)F(\theta^{-1}) + O\left(\frac{e^2}{\hbar v}\right)^2\right] \quad (36)$$

with $\theta = \omega_B/vq_c$. Again, α is the probability for the fast electron in a bulk sample to excite a bulk plasmon during a collision, i.e., α is the ratio of the total lifetime and the lifetime due to the excitation of the bulk plasmon. The function $F(\theta^{-1})$ is defined as $(1/\pi)\int_0^{\theta^{-1}}(dy/y)\ln|(1+y)/(1-y)|$ which is a smooth function of θ^{-1} varying from $\frac{1}{4}\pi$ for $\theta^{-1}=1$ to $\frac{1}{2}\pi$ for $\theta^{-1}=\infty$.

To obtain the net correction by the modification of the electron self-energy due to bulk-plasmon excitation, we have to combine diagram 6(b) with 6(c) which can be worked out easily due to the local character of the self-energy Σ_a:

$$j_{0(c)}(P,R;\Omega) = -ep|M|^2 \int d\omega \int d^3\vec{r}\, e^{i\vec{p}_\perp\cdot\vec{r}} \int d^3\vec{X}\,\theta(-X) \int d^3\vec{x} A_{00}(\omega,X) G(\vec{X},\vec{x};\Omega+\omega+i\eta)$$
$$\times \frac{i}{2\tau} G(\vec{x},R+\tfrac{1}{2}\vec{r};\Omega+\omega+i\eta) G(R-\tfrac{1}{2}\vec{r},\vec{X};\Omega+\omega-i\eta)\theta(x-X) + \text{c.c}$$
$$= B\delta(P-(\Omega-\Delta+\beta\omega_B-v)^{1/2})\{\alpha\}. \quad (37)$$

Therefore, summing up Eqs. (36) and (37), we find that the correction due to the bulk plasmon will enhance the strength of the main satellite by an amount of

$$\Delta j_{0B}(P,R;\Omega) = B\delta(P-(\Omega-\Delta+\beta\omega_B-v)^{1/2})\left[-\frac{1}{\pi}\frac{e^2}{\hbar v}\left(1-\frac{1}{\epsilon}\right)\left(\ln\left|\frac{1+\theta}{1-\theta}\right| - \frac{\pi}{2}F(\theta^{-1})\right)\right] . \quad (38)$$

The total strength of the main peak $j_0(P,R,\Omega)$ can be obtained by adding Δj_{0B} and Δj_{0S} [Eq. (33)] to j_{00} [Eq. (B1)]. We have

$$j_0(P,R;\Omega) = j_{00}(P,R;\Omega) + \Delta j_{0B}(P,R;\Omega) + \Delta j_{0S}(P,R;\Omega)$$
$$\simeq B\delta(P-(\Omega-\Delta+\beta\omega_B-v)^{1/2})\left[1+\frac{1}{2}\frac{e^2}{\hbar v}\left(1-\frac{1}{\epsilon}\right)F(\theta^{-1}) - \frac{\pi}{2}\frac{e^2}{\hbar v}\left(\frac{\epsilon-1}{\epsilon+1}\right)\right.$$
$$\left. - \frac{1}{\pi}\frac{e^2}{\hbar v}\left(1-\frac{1}{\epsilon}\right)\ln\left|\frac{1+\theta}{1-\theta}\right| + \frac{e^2}{\hbar v}\left(\frac{\epsilon-1}{\epsilon+1}\right)\left(\tan^{-1}\theta_S + \frac{\theta_S}{1+\theta_S^2}\right)\right] . \quad (39)$$

It is clear that the modifications of the strength of the peaks in the spectrum due to the higher-order corrections of the electron self-energy are of order $(e^2/\hbar v)^2$ or higher; therefore, we will not consider them.

We now consider the plasmon effects associated with the escape of the fast electron. We are going to calculate diagrams shown in Fig. 7. Again the wavy lines with wave vector $\vec{q}_\parallel$ are surface-plasmon propagators and those with wave vector $\vec{q}$ are bulk-plasmon propagators. So diagram 7(a) contributes to the first surface-plasmon satellite; diagram 7(b) contributes to the first bulk-plasmon satellite, while diagrams 7(c)–7(i) give corrections to the strength of the first bulk-plasmon satellite up to order $e^2/\hbar v$. First, we calculate the strength of the first surface-plasmon satellite $j_S(P,R,\Omega)$. Using the same method which we used to calculate diagrams in Fig. 6, we find that diagram 7(a) gives for the strength of the first surface-plasmon satellite

$$j_S(P,R;\Omega) = B\delta(P-(\Omega-\Delta+\beta\omega_B-v-\omega_S))^{1/2}$$
$$\times \frac{\pi}{2}\frac{e^2}{\hbar v}\left(\frac{\epsilon-1}{\epsilon+1}\right)\left(1-\frac{2}{\pi}\tan^{-1}\theta_S - \frac{2}{\pi}\frac{\theta_S}{1+\theta_S^2}\right) . \quad (40)$$

This is the same as Δj_{0S} [Eq. (33)] except the differences in signs and the momentum shifts. We obtain the expression for the strength ratio of the first surface-plasmon satellite and the main peak by dividing Eq. (40) by Eq. (39) and ignoring the difference in energy shifts. We have

$$\frac{j_S(R,\Omega)}{j_0(R,\Omega)} = \frac{\pi}{2}\frac{e^2}{\hbar v}\left(\frac{\epsilon-1}{\epsilon+1}\right)$$
$$\times\left(1-\frac{2}{\pi}\tan^{-1}\theta_S - \frac{2}{\pi}\frac{\theta_S}{1+\theta_S^2}\right) + O\left(\frac{e^2}{\hbar v}\right)^2 \quad (41)$$

with

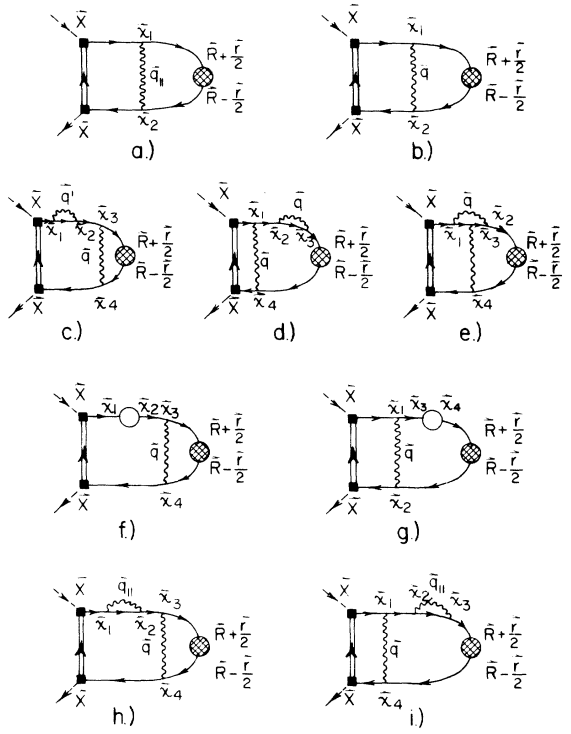

FIG. 7. All the diagrams which contribute to the strength of the first surface/bulk-plasmon satellite up to order $e^2/\hbar v$ due to the plasmon excitation by the escaping photoelectron. Diagrams (a) and (b) contribute respectively to the strength of the first surface- and bulk-plasmon satellite whereas (c)–(i) give correction to the strength of the first bulk-plasmon satellite by modifying the photoelectron's self-energy and by vertex correction.

$$j(R,\Omega)\equiv d\Omega\,(\theta\sim 0,\psi)\int p^2 dp\, j(\vec{P},R,\Omega).$$

For metal, we have $\epsilon\to\infty$, this is the same result obtained by Stern and Ferrell[17] for energy loss of a high-energy electron incident normally on a semi infinite metal. In their case the fast electron is sent in from outside and goes on and on to excite a surface plasmon, while in our case the electron is created somewhere inside the solid (for those electrons escaping without doing other things such as exciting a bulk plasmon or electron-hole pairs, the average position at which they are created is about a distance l inside the surface) and is detected outside the sample. In case the skin depth of the sample δ and the inelastic escape depth l are infinitely large, the results for the two cases should be the same. However, for finite δ and l one expects a difference of order

$$O(lq_c)^{-1}+O(\delta q_c)^{-1}\sim O(lq_c)^{-1}\sim O(e^2/\hbar v)^2.$$

This is a correction of order higher than that we are interested, and this explains why we get the same result at order $e^2/\hbar v$ for the strength of the first surface-plasmon satellite for these two experiments.

For the strength of the first bulk-plasmon satellite we consider first diagram 7(b) which gives

$$j_{B(b)}(P,R,\Omega)=B\delta(P-(\Omega-\Delta+\beta\omega_B-v-\omega_B)^{1/2})\times\left[\alpha-\frac{1}{2}\frac{e^2}{\hbar v}F(\theta^{-1})\left(1-\frac{1}{\epsilon}\right)+\frac{1}{\pi}\frac{e^2}{\hbar v}\left(1-\frac{1}{\epsilon}\right)\ln\left|\frac{1+\theta}{1-\theta}\right|\right]. \quad (42)$$

Again, this is the same as Eq. (36) except the differences of the signs and the momentum shifts.

Diagrams 7(c), 7(d), 7(f), and 7(g) give corrections to the strength of the first bulk-plasmon satellite due to the modification of the localized fast-electron self-energy Σ_a by the bulk plasmons, while diagram 7(e) gives corrections to the strength due to the electron-plasmon vertex correction. It is easier for us to calculate diagrams 7(c)–7(e) together instead of calculating them separately. We find that the contribution to the first bulk-plasmon satellite due to these three diagrams and their complex conjugate is

$$\Delta j_{B(c,d,e)}(P,R;\Omega)=B\delta(P-(\Omega-\Delta+\beta\omega_B-v-\omega_B)^{1/2})\times(-\alpha)\left[\alpha-\frac{1}{2}\frac{e^2}{\hbar v}\left(1-\frac{1}{\epsilon}\right)F(\theta^{-1})+\frac{1}{\pi}\frac{e^2}{\hbar v}\left(1-\frac{1}{\epsilon}\right)\ln\left|\frac{1+\theta}{1-\theta}\right|\right]; \quad (43)$$

whereas diagrams 7(g) and 7(f) and their complex conjugate give for the strength of the first plasmon satellite a correction of

$$\Delta j_{B(g,f)}(P,R;\Omega)=B\delta(P-(\Omega-\Delta+\beta\omega_B-v-\omega_B)^{1/2})\times(\alpha)\left[\alpha-\frac{1}{2}\frac{e^2}{\hbar v}\left(1-\frac{1}{\epsilon}\right)F(\theta^{-1})+\frac{1}{\pi}\frac{e^2}{\hbar v}\left(1-\frac{1}{\epsilon}\right)\ln\left|\frac{1+\theta}{1-\theta}\right|\right]. \quad (44)$$

This cancels $\Delta j_{B(c,d,e)}$ exactly up to order of $e^2/\hbar v$.

The corrections to the first bulk-plasmon satellite by modifying the fast-electron self-energy due to the surface-plasmon excitations are given by diagrams 7(h) and 7(i) and their complex conjugates. They give

$$\Delta j_{B(h,i)}=B\delta(P-(\Omega-\Delta+\beta\omega_B-V-\omega_B)^{1/2})\times\left[-\alpha\frac{\pi}{2}\frac{e^2}{\hbar v}\left(\frac{\epsilon-1}{\epsilon+1}\right)\times\left(1-\frac{2}{\pi}\tan^{-1}\theta_s-\frac{2}{\pi}\frac{\theta_s}{1+\theta_s^2}\right)\right]. \quad (45)$$

Therefore the total strength of the first bulk-plasmon satellite due to the extrinsic effect $j_B(P,R,\Omega)$ can be obtained by summing up Eqs. (42)–(45). We have

$$j_B(P,R;\Omega)\equiv j_{B(b)}(P,R,\Omega)+\Delta j_{B(c-i)}(P,R;\Omega)$$

$$=B\delta(P-(\Omega-\Delta+\beta\omega_B-v-\omega_B)^{1/2})\left[\alpha+\frac{1}{\pi}\frac{e^2}{\hbar v}\left(1-\frac{1}{\epsilon}\right)\ln\left|\frac{1+\theta}{1-\theta}\right|\right.$$

$$\left.-\frac{1}{2}\frac{e^2}{\hbar v}\left(1-\frac{1}{\epsilon}\right)F(\theta^{-1})-\alpha\frac{\pi}{2}\frac{e^2}{\hbar v}\left(\frac{\epsilon-1}{\epsilon+1}\right)\left(1-\frac{2}{\pi}\tan^{-1}\theta_S-\frac{2}{\pi}\frac{\theta_S}{1+\theta_S^2}\right)\right]. \quad (46)$$

From Eqs. (46) and (39) the strength ratio of this first bulk-plasmon satellite and the main peak (due to the "extrinsic" terms alone) can be shown to be

$$\frac{j_B(R,\Omega)}{j_0(R,\Omega)}=\alpha+\frac{1+\alpha}{\pi}\frac{e^2}{\hbar v}\left(1-\frac{1}{\epsilon}\right)\ln\left|\frac{1+\theta}{1-\theta}\right|$$

$$-\frac{1+\alpha}{2}\frac{e^2}{\hbar v}\left(1-\frac{1}{\epsilon}\right)F(\theta^{-1}). \quad (47)$$

We recall that $\theta=\omega_B/vq_c\ll 1$ and $F(\theta^{-1})$ is a smooth function which varies from $\frac{1}{2}\pi$ for $\theta=0$ to $\frac{1}{2}\pi$ for $\theta=1$.

Before we compare this result with that obtained in I, we notice that the second term on the right-hand side of Eq. (47) is small, although formally it is of order $e^2/\hbar v$, because $\omega_B/vq_c\sim v_f/v\sim[(1\text{ Ry})/E]^{1/2}\sim e^2/\hbar v$, making the logarithm small and the factor $1/\pi$ in front makes the term even smaller. Therefore we neglect it in making the comparison. In I, we found that, for a bulk sample the strength ratio of the first plasmon satellite and the main peak [Eq. (10) of I] is

$$j_B/j_0=\alpha \text{ for bulk sample,} \quad (48)$$

and all corrections to this are either of form $(1/\pi)(e^2/\hbar v)\ln|(1+\theta)/(1-\theta)|$ [Eqs. (20)–(24) of I] or of higher order, and thus negligible in the same spirit as above. Therefore the surface effect on the strength ratio of the first bulk-plasmon satellite to the main peak due to the plasmon excitations by the escaping photoelectrons is to *reduce* the strength ratio by an amount of

$$\frac{1+\alpha}{2}\frac{e^2}{\hbar v}\left(1-\frac{1}{\epsilon}\right)F\left(\frac{vq_c}{\omega_B}\right). \quad (49)$$

This is of the same order as that of the first surface-plasmon satellite [Eq. (41)] although, for larger ϵ, (49) is smaller.

V. INTERFERENCE TERMS

In this section we show that the interference terms and vertex corrections correlated in I are unchanged by the surface to the order of our calculation. Refer now to Fig. 8; diagram 8(a) can be considered as either an interference term or a vertex correction depending on whether the final state has a plasmon excited or not. Taking both cases into consideration, we have for diagram 8(a)

$$-2ep|M|^2\int d\omega\int d^3\vec{r}\,e^{i\vec{q}_\perp\cdot\vec{r}}\int d^3\vec{X}\int d^3\vec{x}\,\theta(x-X)\theta(-x)$$

$$\times\sum_{\vec{q}}g_{qB}^2\sin q_\perp x\sin q_\perp X\,e^{-i\vec{q}_\parallel\cdot(\vec{X}-\vec{x})}G(\vec{X},\vec{x};\Omega+\omega+i\eta)\,G(\vec{x},R+\tfrac{1}{2}\vec{r};\Omega+\omega+\omega_B+i\eta)\,G(R-\tfrac{1}{2}\vec{r},\vec{X};\Omega+\omega-i\eta)$$

$$\times[A(\omega+\omega_B,X)g_h(\omega-i\eta;\vec{X})+A(\omega,X)g_h(\omega+\omega_0-i\eta,\vec{X})], \quad (50)$$

where $g_h(\omega,X)$ is the Fourier transform of the deep-hole Green's function $g_h(t,X)$ [Eq. (19)],

$$g_h(\omega,X)=\theta(-X)/(\omega+\Delta-i\eta). \quad (51)$$

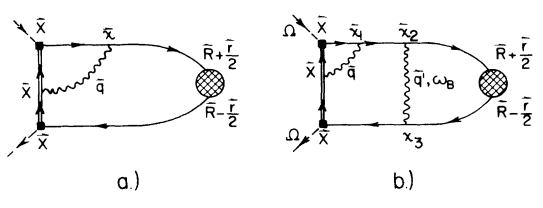

FIG. 8. Interference diagrams which contribute to the strengths of the main and first bulk-plasmon satellites by an amount of order $e^2/\hbar v$.

By using the same approximation for calculating the extrinsic effects (50) reduces to

$$B\frac{e^2}{\hbar v}\left(1-\frac{1}{\epsilon}\right)F(\theta^{-1})[\delta(P-(\Omega-\Delta+\beta\omega_B-v)^{1/2})$$

$$-\delta(P-(\Omega-\Delta+\beta\omega_B-v-\omega_B)^{1/2})]. \quad (52)$$

Thus, as in bulk case this enhances the main peak by a fraction of

$$(e^2/\hbar v)(1-1/\epsilon)F(\theta^{-1}) \quad (53)$$

and reduces the strength of the first bulk-plasmon satellite by the same amount. This result is the same as that obtained in I [Eq. (29) of I]. The other interference diagram which modifies the first bulk-plasmon satellite is diagram 8(b). This

process involves the excitation of a real bulk plasmon by the escaping fast electron; therefore, the average position that the photoelectrons are excited is a distance of l further inside the solid surface compared to that of diagram 8(a). So we expect the surface corrections to diagram 8(b) are smaller than that to diagram 8(a) and hence have no correction up to order $e^2/\hbar v$ at all. Thus diagram 8(b) and its complex conjugate reduce the strength of the second bulk-plasmon satellite by an amount of $\alpha(e^2/\hbar v)F(\theta^{-1})$ and add them to the strength of the first bulk-plasmon satellite. We conclude that the presence of the surface has no effect on the interference corrections.

We will not consider the surface effect on the strength of the second or higher plasmon satellites. Again this is because those photoelectrons which contribute to these satellites are originated at positions deeper inside the solid than those of the main and first plasmon satellite. Therefore the surface on these satellites will not be larger than that of the first two. We discuss the case of detecting the photoelectrons at an angle of θ with respect to the normal of the solid surface in Appendix E.

APPENDIX A

In Refs. 6 and 10 only one form of multiplasmon interaction with the deep hole was considered, although the methods for handling the general problem were discussed. Specifically the only multiple plasmon interaction worked out there, and indeed the only one included in our model Hamiltonian in this paper, is in the form of a repeated one plasmon interaction. The purpose of this appendix is to justify this approximation by explicitly calculating the lowest-order two plasmon vertex for long wavelengths and showing that it is small.

The diagrams to be calculated are of the form in Figs. 9(a) and 9(b); the sum of 9(a) and 9(b) is to be multiplied by 2 to account for the two similar diagrams with the triangular vertex on the right; note that in each case we will ultimately consider that part of the diagram which contributes weight to the second plasmon satellite, and this is indicated by the dotted line across the diagram. We first calculate the triangular three prong vertex composed of the three electronic Green's functions. This is most easily done at finite temperatures by performing the Matsubara sum and then taking the $T=0$ limit; these steps are done by inspection with the result

$$\sum_{p,\sigma}\left[\frac{f_{p-q_2}}{(\omega_1+\omega_2+\epsilon_{p-q_2}-\epsilon_{p+q_1})(\omega_2+\epsilon_{p-q_2}-\epsilon_p)}+\frac{f_{p+q_1}}{(-\omega_1-\omega_2+\epsilon_{p+q_1}-\epsilon_{p-q_2})(-\omega_1-\epsilon_{p+q_1}-\epsilon_p)}+\frac{f_p}{(\omega_1+\epsilon_p-\epsilon_{p+q_1})(\epsilon_p-\omega_2-\epsilon_{p-q_2})}\right], \tag{A1}$$

where $\epsilon_p=P^2/2m$, ω_1, ω_2, q_1, and q_2 are defined as in Fig. 9. Since q_1 and q_2 are plasmon wave vectors, and hence limited in magnitude, we may obtain a reasonable approximation to (A1) by expanding in powers of q_1 and q_2, with the result that (A1) is approximately given by

$$\frac{n}{16m^2\omega_p^4}\left[(\vec{q}_1+\vec{q}_2)^4-2(q_1^4+q_2^4)+(\vec{q}_1+\vec{q}_2)^2(q_1^2+q_2^2)+4q_1^2q_2^2\right]\equiv\alpha_{q_1,q_2}, \tag{A2}$$

where n is the number of electrons per unit volume and where we have set $\omega_1=\omega_2=\omega_p$, in anticipation of insisting on the two plasmon "final" state. Actually there is a term of lower order of the form $q_1^2-q_2^2$, but this will be exactly canceled by a term of opposite sign when we eventually sum the contributions from 9(a) and 9(b) [note that 9(b) may be obtained from 9(a) by interchanging (q_1,ω_1) with (q_2,ω_2)]. The contribution to the weight of the second plasmon satellite of 9(a) is

$$\frac{1}{\omega_p}\frac{1}{(2\omega_p)^2}\sum_{\vec{q}_1,\vec{q}_2}\frac{4\pi e^2}{(\vec{q}_1+\vec{q}_2)^2}|q_{q_1}|^2|q_{q_2}|^2\alpha_{q_1,q_2}, \tag{A3}$$

where we have replaced the wavy line on the left of 9(a) by the bare Coulomb interaction, because the screening or antiscreening effect at twice the plasma frequency and small q must necessarily be small. Upon performing the straightforward but tedious integrations, and multiplying by 4 to account for 9(b), plus the fact that in either 9(a) or 9(b) the imaginary part may be taken with the triangular vertex either to the right or the left of the two plasmon states, we find that the total contribution of this kind to the weight of the second plasmon satellite is

$$\tfrac{1}{16}(2-\tfrac{1}{8}\pi^2)(q_c^2/m\omega_p)\beta^2. \tag{A4}$$

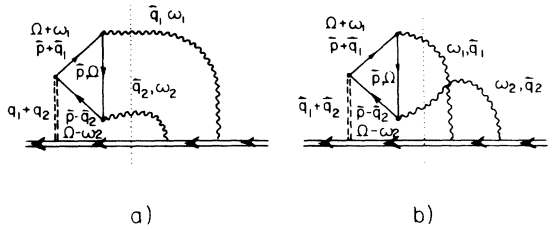

FIG. 9. Contributions to the second plasmon satellite which are not included in the basic approximations in this paper. As shown in Appendix A their contribution is small. The double dashed line represents the full dynamically shielded Coulomb interaction, which may be approximated by the bare Coulomb interaction when the imaginary part is taken (as indicated by the dotted line) when two plasmons are present.

However, the strength of the second plasmon satellite due to Fig. 3 for bulk case is just $\frac{1}{2}\beta^2$—note that these are the contributions included in the approximations of the main body of the paper. Taking $q_c = \omega_p/v_f$, we find that the ratio of (A4) to $\frac{1}{2}\beta^2$ is approximately

$$0.06(\tfrac{1}{2}r_s)^{1/2}, \tag{A5}$$

where r_s is the usual electron gas spacing parameter in atomic units. Thus (A5) represents a very small percentage correction r_s in the range of normal metals $2 \lesssim r_s \lesssim 5$. A further point to notice is that (A4) is proportional to q_c^4 while $\frac{1}{2}\beta^2$ is proportional only to q_c^2. This means that on the average the plasmons contributing to (A4) have larger wave vectors than those contributing to $\frac{1}{2}\beta^2$, so that they will be more highly damped. Therefore we expect terms of this type to make a small and highly smeared out contribution to the satellite.

APPENDIX B: EFFECT ON $\delta K(X)$ ON THE STRENGTH OF THE MAIN PEAK

To obtain the strength of the main peak, we use $A_{00}(\omega, X)$ [Eq. (27)] for the deep-hole spectral density $A(\omega, X)$ in Eq. (11), which after being integrated over ω gives for the photocurrent from the electrons contributing to the main peak the expression

$$j_{00}(P, R, \Omega) = -2ep|M|^2 \int_{-\infty}^{0} dX \times \frac{e^{K(X)+X/l}\,\delta(P - (\Omega - \Delta - \Delta E(X) - V)^{1/2})}{4(\Omega - \Delta - \Delta E(X))}. \tag{B1}$$

This gives for the strength of the main peak

$$\begin{aligned} j_{00}(R, \Omega) &= d\Omega(\theta \sim 0, \psi) \int P^2 dP\, j_{00}(P, R, \Omega) \\ &= -2e|M|^2 \int_{-\infty}^{0} dX \times \frac{e^{K(X)+X/l}[\Omega - \Delta - \Delta E(x) - V]^{3/2}}{4[\Omega - \Delta + \Delta E(x)]}\, d\Omega(\theta \sim 0, \psi) \\ &\simeq -\frac{e|M|^2 v}{4}\, d\Omega(\theta \sim 0, \psi) \int_{-\infty}^{0} dX\, e^{K(X)+X/l}. \end{aligned} \tag{B2}$$

To obtain Eq. (B2) we have neglected the position dependence of the energy shift and the constant potential energy V which we have shown to lead to a correction of order (1 Ry)/E or higher, where E is the energy of the photoelectron.

If we neglect $\delta K(X)$ completely Eq. (B2) becomes

$$j_{00}(R; \Omega;\ \delta K(X) = 0) = \tfrac{1}{4} B v^2 d\Omega(\theta \sim 0, \psi), \qquad B \equiv -e|M|^2 e^{-\beta} l/v. \tag{B3}$$

Taking $\delta K(X)$ into consideration, instead of B we obtain $B + \delta B$ for the strength of the main peak, where

$$\delta B/B = \frac{1}{l} \int_{-\infty}^{0} dX\, e^{\delta K(X)+X/l} - 1. \tag{B4}$$

Although the integral in (B3) cannot be worked out analytically, it can be shown to be small. We divide the domain of the integration into two parts, i.e.,

$$\int_{-\infty}^{0} = \int_{-\infty}^{-q_c^{-1}} + \int_{-q_c^{-1}}^{0-1}. \tag{B5}$$

In each part we use for $\delta K(X)$ its appropriate asymptotic forms. From Eqs. (22), (23), and (27) we have

$$\begin{aligned} \delta K(X) &= -\frac{e^2 q_c}{2\omega_s}\left(\frac{\epsilon - 1}{\epsilon + 1}\right)(1 + q_c X) + \beta\left(1 - \frac{1}{\epsilon}\right) \quad \text{if } |x| \ll q_c^{-1} \\ &= -\frac{e^2}{4X}\,\frac{1}{\omega_B}\left(1 - \frac{1}{\epsilon}\right) - \frac{1}{\omega_S}\left(\frac{\epsilon - 1}{\epsilon + 1}\right) \quad \text{if } |x| \gg q_c^{-1}. \end{aligned} \tag{B6}$$

By using (B5), it is easy to show that the leading terms for the integrals at the right-hand side of (B4) are

$$\begin{aligned} \int_{-\infty}^{-q_c^{-1}} &\sim e^{-1/q_c l} + \frac{e^2}{4l}(\ln q_c l)\left[\frac{1}{\omega_B}\left(1 - \frac{1}{\epsilon}\right) - \frac{1}{\omega_S}\left(\frac{\epsilon - 1}{\epsilon + 1}\right)\right] \\ &\sim 1 + O\left(\frac{1}{lq_c}\right), \end{aligned} \tag{B7}$$

$$\int_{-q_c^{-1}}^{0^-} \lesssim \frac{1}{l}\int_{-q_c^{-1}}^{0^-} dX e^{\beta(1-1/\epsilon)} \sim O\left(\frac{1}{lq_c}\right).$$

Therefore the effect of $\delta K(X)$ on the strength of the main peak, from Eq. (B3), is of order $(lq_c)^{-1} \sim (e^2/\hbar v)(\omega_B/vq_c)\ln(mv^2/\omega_B)$. Since $\omega_B/vq_c \sim v_f/v \sim [(1\text{ Ry})/E]^{1/2} \sim e^2/\hbar v$, this correction, although has form of order $e^2/\hbar v$, is actually of order $(e^2/\hbar v)^2$ and hence can be neglected.

APPENDIX C: SURFACE-PLASMON SATELLITE DUE TO THE INTRINSIC EFFECT

To obtain the strength of the first surface-plasmon satellite due to the readjustment of the Fermi gas to the deep-hole potential we use in Eq. (11) for the deep-hole spectral density

$$A_{01}(\omega, X) = e^{K(X)} \sum_{\vec{q}_\parallel} \frac{q_{qS}^2}{\omega_S^2}\, e^{-2|\vec{q}_\parallel||X|} \times \theta(-X)\,\delta(\omega - \Delta - \omega_S - \Delta E(X)). \tag{C1}$$

After being integrated over ω, Eq. (11) gives

$$j(P, R, \Omega) = -2ep|M|^2 \int_{-\infty}^{0} dX \frac{e^{K(X)}\beta_S(X)\, e^{X/l}}{4[\Omega - \Delta - \omega_S - \Delta E(x)]} \times \delta(P - [\Omega - \Delta - \omega_S - \Delta E(x)]^{1/2}). \tag{C2}$$

So, the total strength of the satellite in question,

$j(R, \Omega)$, is given by

$$j(R,\Omega) \simeq -\tfrac{1}{4} e\,|M|^2 v\, d\Omega(\theta\sim 0,\psi)\int_{-\infty}^{0} dX\, e^{K(X)+X/l}\beta_S(X). \tag{C3}$$

Again, as in Appendix B, we separate the domain of the integration into two parts and in each part we use for $K(X)$ and $\beta_S(X)$ their appropriate asymptotic expressions which can be obtained from Eqs. (22), (23) and (25). We have

$$\begin{aligned} &-\frac{e\,|M|^2 v}{4}\, d\Omega(\theta\sim 0,\psi)\int_{-\infty}^{-q_c^{-1}} dX\, e^{K(X)+X/l}\beta_S(X) \\ &\sim \frac{Bv^2}{4}\,\frac{e^2}{4l}\,\frac{1}{\hbar\omega_S}\,\ln(lq_c)\, d\Omega(\theta\sim 0,\psi) \\ &\sim \frac{Bv^2}{4}\, d\Omega(\theta\sim 0,\psi)\left\{O\left(\frac{e^2}{\hbar v}\right)^2\right\} \end{aligned} \tag{C4}$$

and

$$\begin{aligned} &-\frac{e\,|M|^2 v}{4}\, d\Omega(\theta\sim 0,\psi)\int_{-q_c^{-1}}^{0} dX\, e^{K(X)+X/l}\beta_S(X) \\ &\lesssim \frac{Bv^2}{4}\, d\Omega(\theta\sim 0,\psi)(e^{\delta K}\beta_s)_{\max}\,\frac{1}{q_c l} \\ &\sim \frac{Bv^2}{4}\, d\Omega(\theta\sim 0,\psi)\left\{O\left(\frac{e^2}{\hbar v}\right)^2\right\}, \end{aligned}$$

where $(e^{\delta K}\beta_s)_{\max}$ is the maximum value of $e^{\delta K(X)}\beta_S(X)$ for $-q_c^{-1}\le x\le 0$. It is of order $[e^{\delta K(X)}\beta_S(X)]_{x=0} \sim e^2 q_c/\hbar\omega_S|$.

APPENDIX D

One may be interested to see how important is the correction of the fast-electron self-energy to the spectral line. If we take the localized self-energy $\Sigma_a(\vec{r},\vec{r}';\omega\pm i\eta)$ [Eq. (4)] as the true self-energy for the photoelectrons, we have, for the strength of the main peak $j_0(R,\Omega)$ only $j_{00}(R,\Omega)$ [Eq. (B3)]; and for the strength of the first bulk-plasmon satellite due to the extrinsic effects $j_B(R,\Omega)$, we have only $j_{B(b)}(R,\Omega)$ [Eq. (42)] and $j_{B(e)}(R,\Omega)$. We obtain $j_{B(e)}(R,\Omega)$ by calculating diagram 7(e) and its complex conjugate. We find

$$\begin{aligned} j_{B(e)}(P,R;\Omega) &= B\,\delta(P-(\Omega-\Delta+\beta\omega_B-V-\omega_B)^{1/2}) \\ &\times\left[\frac{\alpha}{\pi}\,\frac{e^2}{\hbar v}\left(1-\frac{1}{\epsilon}\right)\ln\left|\frac{1+\theta}{1-\theta}\right|\right]. \end{aligned} \tag{D1}$$

Therefore the new strength ratio becomes

$$\begin{aligned} \frac{j_B(R,\Omega)}{j_0(R,\Omega)} &\equiv \frac{j_{B(b)}(R,\Omega)+j_{B(e)}(R,\Omega)}{j_{00}(R,\Omega)} \\ &\simeq \alpha-\frac{1}{2}\,\frac{e^2}{\hbar v}\left(1-\frac{1}{\epsilon}\right)F(\theta^{-1}) \\ &+\frac{1+\alpha}{\pi}\,\frac{e^2}{\hbar v}\left(1-\frac{1}{\epsilon}\right)\ln\left|\frac{1+\theta}{1-\theta}\right| \\ &\text{(local self-energy approximation).} \end{aligned} \tag{D2}$$

The difference between this and (47) is

$$\frac{\alpha}{2}\,\frac{e^2}{\hbar v}\left(1-\frac{1}{\epsilon}\right)F(\theta^{-1}) < \frac{\alpha}{2}\,\frac{e^2}{\hbar v}\left(1-\frac{1}{\epsilon}\right)\frac{\pi}{2}\ , \tag{D3}$$

which, for metal with $\alpha=\frac{1}{2}$, is smaller than $\frac{1}{8}\pi(e^2/\hbar v)<5\%$ for 15-keV photoelectrons. Since the surface-plasmon effects are of order $e/\hbar v$ and the corrections due to the modification of the fast-electron self-energy are of order $e^2/\hbar v$ also, the effect of the latter on the surface-plasmon satellite is of order $(e^2/\hbar v)^2$ and therefore can be neglected. Thus, the local self-energy approximation seems not bad at all for high-energy photoelectrons.

APPENDIX E

We consider the case of detecting the photoelectrons at angles θ, ψ away from the normal of the surface. Of course, the deep-hole spectral density does not change. Following the same way as for the normal case (i.e., $\theta=0$) we find the corresponding value for $j_{00}(P,R,\omega)$ to be

$$\begin{aligned} j_{00}(P,R,\Omega,\theta) &= -\frac{ep_\perp|M|^2 e^{-\beta l}\cos\theta}{v^2\cos^2\theta} \\ &\times\delta(P_\perp-(\Omega-\Delta-V+\beta\omega_B-p_\parallel^2)^{1/2}) \end{aligned} \tag{E1}$$

and the strength of main peak becomes

$$\begin{aligned} j_{00}(R,\Omega,\theta) &= d\Omega(\theta,\psi)\int p^2 dp\, j_{00}(P,R,\Omega,\theta) \\ &= \tfrac{1}{4}B\cos\theta\, v^2 d\Omega(\theta,\psi), \end{aligned} \tag{E2}$$

where $d\Omega(\theta,\psi)$ is the small solid angle around θ,ψ. This is smaller than that of the normal case by a factor of $\cos\theta$ (if M is independent on θ). The reason for this is that for the normal case, the escaping electrons, on the average, originate at a distance l inside the surface, while for electrons escaping with an angle θ to the surface normal, the positions they originate from are, on the average, only $l\cos\theta$ inside the surface. Since the total number of core electron states in volume Sl is larger by a factor of $\cos\theta$ than those in volume Sl and, where S is the surface area, there are a factor of $\cos\theta$ more electrons to be able to escape in the former case than that in the latter case.

Now we consider the diagrams involving only one plasmon propagator. We calculated diagram 6(a) and found it to be given by

$$\begin{aligned} j_{0S}(P,R,\Omega,\theta) &= \frac{ep_\perp|M|^2 e^{-\beta l_\perp}}{v^2\cos^2\theta}\sum_{\vec{q}_\parallel}\frac{g_{qS}^2\,\delta(P_\perp-(\Omega-\Delta+\beta\omega_B-v-p_\parallel^2))}{v^2-v_\parallel^2-\vec{v}\cdot\vec{q}_\parallel} \\ &\times\left(\frac{4q_\parallel^2}{\{q_\parallel^2+[(\omega_S-\vec{v}\cdot\vec{q}_\parallel)/v_\perp]^2\}^2}+\frac{1}{q_\parallel^2+[(\omega_s-\vec{v}\cdot\vec{q}_\parallel)/v_\perp]^2}\,\frac{1}{2|q_\parallel|+l_1^{-1}}\right. \end{aligned}$$

$$-\frac{4q_{\parallel}^2(q_{\parallel}+l_{\perp}^{-1})+4q_{\parallel}[(\omega_S-\vec{v}\cdot\vec{q}_{\parallel})/v_{\perp}]^2}{\{q_{\parallel}^2+[(\omega_S-\vec{v}_{\parallel}\cdot\vec{q})/v_{\perp}]^2\}^2\{[(\omega_S-\vec{v}_{\parallel}\cdot\vec{q})/v_{\perp}]^2+(|q_{\parallel}|+l_{\perp}^{-1})^2\}}\Bigg) \tag{E3}$$

with $v_{\perp}=v\cos\theta$ and $l_{\perp}=l\cos\theta$. The quantity in the large parentheses is the same as that in (32) except the replacement of ω_S by $\omega_S-\vec{v}_{\parallel}\cdot\vec{q}_{\parallel}$ and v by $v_{\perp}$, if we let, in the denominator, $v^2-v_{\parallel}^2-\vec{v}_{\parallel}\vec{q}_{\parallel}\sim v_{\perp}^2$. This approximation neglects a correction to the strength of the satellite by a fraction of $\vec{v}_{\parallel}\cdot\vec{q}_{\parallel}/v_{\perp}^2\lesssim q_c/v_{\perp}\sim e^2/\hbar v$ (for $v_{\parallel}\leq v_{\perp}$). Since the strength of the surface-plasmon satellite itself is of order $e^2/\hbar v$ and we are interested in quantities of this order, it is reasonable to make this approximation. Again the important contribution comes from the first term in the large parentheses which can be shown by a straightforward but tedious calculation to give the contribution to $j_{0S}(P,R,\Omega,\theta)$:

$$j_{0S}(P,R,\Omega,\theta)=\frac{ep_{\perp}|M|^2e^{-\beta}l\cos\theta\,\delta(P_{\perp}-(\Omega-\Delta+\beta\omega_B-V-p_{\parallel}^2)^{1/2})}{(v^2\cos^2\theta)^2}$$
$$\times\left(\frac{\epsilon-1}{\epsilon+1}\right)\Bigg\{-\frac{e^2v_{\perp}}{4i}\frac{\partial}{\partial v_{\perp}}\frac{1}{v_{\perp}}\ln\left[\left(\frac{\omega_S+iv_{\perp}q_c}{\omega_S-iv_{\perp}q_c}\right)^2\right.$$
$$\left.\times\frac{i-\{-1+[v_{\parallel}q_c/(\omega_S^2+v_{\perp}^2q_c^2)](\omega_S^2-v_{\perp}^2q_c^2)-2iv_{\perp}v_{\parallel}^2q_c^3\omega_s/(\omega_S^2+v_{\perp}^2q_c^2)^2\}}{i+\{-1+[v_{\parallel}q_c/(\omega_S^2+v_{\perp}^2q_c^2)](\omega_S^2-v_{\perp}^2q_c^2)-2iv_{\perp}v_{\parallel}^2q_c^3\omega_S/(\omega_S^2+v_{\perp}^2q_c^2)^2\}}\right]\Bigg\} \tag{E4}$$

with $-\pi<$ argument $<\pi$. If in (E4) we neglect terms which correct the strength of the satellite by a fraction of ω_S/vq_c, Eq. (E4) can be simplified as

$$j_{0S}(P,R,\Omega,\theta)\simeq\frac{ep_{\perp}|M|^2e^{-\beta}l\cos\theta\,\delta(P_{\perp}-(\Omega-\Delta+\beta\omega_B-V-p_{\parallel}^2)^{1/2})}{(v^2\cos^2\theta)^2}\left(\frac{e^2v_{\perp}}{4i}\frac{\partial}{\partial v_{\perp}}\frac{1}{v_{\perp}}2\pi i\right)\left(\frac{\epsilon-1}{\epsilon+1}\right), \tag{E5}$$

which gives for the total strength of the surface-plasmon satellite

$$j_{0S}(R,\Omega;\theta)=-\frac{Bv^2}{4}\cos\theta\,d\Omega(\theta,\psi)\left[\frac{e^2}{\hbar v_{\perp}}\frac{\pi}{2}\left(\frac{\epsilon-1}{\epsilon+1}\right)\right]. \tag{E6}$$

Now, for diagram 6(b), we have

$$j_{0(b)}(P,R,\Omega,\theta)=\frac{ep_{\perp}|M|^2e^{-\beta}l\cos\theta}{2(v^2\cos^2\theta)}\sum_{\vec{q}}\frac{g_{qB}^2}{v^2-v_{\parallel}^2-\vec{v}_{\parallel}\cdot\vec{q}_{\parallel}}\delta(P_{\perp}-(\Omega-\Delta+\beta\omega_B-V-p_{\parallel}^2)^{1/2})$$
$$\times\left[\frac{1}{\{[(\omega_B-\vec{v}_{\parallel}\cdot\vec{q}_{\parallel})/v_{\perp}]+|\vec{q}_{\perp}|\}^2+l_{\perp}^2}+\frac{1}{\{[(\omega_B-\vec{v}_{\parallel}\cdot\vec{q}_{\parallel})/v_{\perp}]-|\vec{q}_{\perp}|\}^2+l_{\perp}^{-2}}-\frac{1}{[(\omega_B-\vec{v}_{\parallel}\cdot\vec{q}_{\parallel})/v_{\perp}]^2-q_{\perp}^2}\right.$$
$$\left.\times\left(1-\frac{1}{l_{\perp}^2}\frac{1}{\{[(\omega_B-\vec{v}_{\parallel}\cdot\vec{q}_{\parallel})/v_{\perp}]+q_{\perp}\}^2+l_{\perp}^{-2}}-\frac{1}{l_{\perp}^2}\frac{1}{\{[(\omega_B-\vec{v}_{\parallel}\cdot\vec{q}_{\parallel})/v_{\perp}]q_{\perp}\}^2+l_{\perp}^{-2}}+\frac{1}{l_{\perp}^2}\frac{1}{4q_{\perp}^2+l_{\perp}^{-2}}\right)\right]. \tag{E7}$$

Again if we take the approximation $v^2-v_{\parallel}^2-\vec{v}_{\parallel}\cdot\vec{q}_{\parallel}\sim v_{\perp}^2$, this is the same expression as Eq. (35) except for the replacement v by $v_{\perp}$, l by $l\cos\theta$, and ω_B by $\omega_B-\vec{v}_{\parallel}\cdot\vec{q}_{\parallel}$. The important contribution comes from the first three terms. Taking the approximation just mentioned the first two terms can be easily evaluated to give a contribution which is a factor of $\cos\theta$ smaller than the first term of Eq. (36) which is contributed by the corresponding terms for the case of normally escaping and hence small. The third term can be rewritten as

$$-\frac{ep_{\perp}^2|M|^2e^{-\beta}l\cos\theta}{2(v\cos\theta)^2}\sum_{\vec{q}}\frac{g_{qB}^2}{(\omega_B-\vec{v}_{\parallel}\cdot\vec{q}_{\parallel})^2-v_{\perp}^2q_{\perp}^2}$$
$$\times\delta(P_q-(\Omega-\Delta+\beta\omega_B-V-p_{\parallel}^2)^{1/2}), \tag{E8}$$

which after the integration on $d^3p=d\Omega(\theta,\psi)\int p^2dp$ gives for the strength of the satellite a contribution

$$\frac{Bv^2\cos\theta}{4}\int_0^1 dy\,\frac{1}{2\pi}\frac{e^2}{\hbar V(y)}\left(1-\frac{1}{\epsilon}\right)\ln\left|\frac{q_cV(y)+\omega_B}{q_cV(y)-\omega_B}\right|, \tag{E9}$$

where $v(y)=[v^2y^2+(1-y)^2v_{\parallel}^2+2y(1-y)\vec{v}\cdot\vec{v}_{\parallel}]^{1/2}$ $=[v_{\perp}^2y^2+v_{\parallel}^2]^{1/2}$. We note that when $v=0$ and $v=v_{\perp}$, (E9) reduces to the value we obtained for the normally escaping electrons. For the interference diagrams, again the expressions are complicated, but there are no corrections due to the finite angle with respect to the normal of the surface up to order $e^2/\hbar v$ (of course again $\theta\leq 45°$, i.e., to assume $|\vec{v}_{\perp}|\leq|\vec{v}_{\perp}|$), except a factor of $\cos\theta$ which modifies

the quantity B and has no effect on the strength ratio. The other one plasmon line diagrams are diagrams 7(a) and 7(b). As before, they have the same contributions, respectively, as diagram 6(a) and 6(b) but with opposite signs. We will not examine higher-order terms because from the previous case of normally escaping we know that the most important contributions to the strength ratio come from these low-order terms, and taking the finite angle into account, those higher-order diagrams give contributions of the same form as that for normally escaping case except to replace l by $l\cos\theta$, v by $v_\perp$, $\omega_{s,B}$ by $\omega_{s,B} - \vec{v}_\parallel \cdot \vec{q}_\parallel$ or $\omega_{s,B} - \vec{v}_\parallel \cdot \vec{q}'_\parallel$; and it will be even harder to evaluate them.

---

*Work supported in part by the National Science Foundation Grant No. GP 29262.

†Preliminary version of this work has appeared: J. J. Chang and D. C. Langreth, Bull. Am. Phys. Soc. **18,** 55 (1973).

‡Present address: Department of Physics, University of California at Santa Barbara, Santa Barbara, Calif. 93106.

[1]For example, see K. Siegbahn, D. Hammond, H. Fellner-Feldegg, and E. F. Barnett, Science **176,** 245 (1972).

[2]R. H. Ritchie, Phys. Rev. **114,** 644 (1959).

[3]D. E. Eastman, in Physical Electronic Conference, Albuquerque, 1972 (unpublished); J. W. T. Ridgway and D. Haneman, Surf. Sci. 24, 451 (1971); Surf. Sci. **26,** 683 (1971); M. L. Tarng and G. K. Wehner, Physical Electronic Conference, Albuquerque, 1972, (unpublished); P. W. Palmberg and T. N. Rhodin, J. Appl. Phys. **39,** 2425 (1968); K. Jacob and H. Hölzl, Surf. Sci. **26,** 54 (1971); R. G. Steinhard, J. Hudis, and M. L. Perlman, *Proceedings of the International Conference on Electron Spectroscopy, Grove, Calif., 1971,* (North-Holland, Amsterdam, 1972), p. 557; Yves Baer *et al.*, Solid State Commun. 8, 1479 (1970).

[4]Essentially that of J. I. Gersten, Phys. Rev. **188,** 774 (1969); see also P. J. Feibelman, C. B. Duke, and A. Bagchi, Phys. Rev. B **5,** 2436 (1972).

[5]This model neglects certain types of multiplasmon creation processes. These are estimated to be small in Appendix A.

[6]J. J. Chang and D. C. Langreth, Phys. Rev. B **5,** 3512 (1972) (hereafter referred to as I).

[7]G. D. Mahan, Phys. Rev. **153,** 822 (1967); Phys. Rev. **163,** 612 (1967).

[8]P. Nozières and C. J. De Dominicis, Phys. Rev. 178, 1097 (1969); D. C. Langreth, Phys. Rev. B **3,** 3120 (1971).

[9]S. Doniach and M. Šunjić, J. Phys. C **3,** 285 (1970).

[10]D. C. Langreth, Phys. Rev. B **1,** 471 (1970).

[11]A. Rosenwaig, G. R. Wertheim, and H. J. Guggenheim, Phys. Rev. Lett. **27,** 479 (1971); G. K. Werthaim and A. Rosenwaig, Phys. Rev. Lett. **26,** 1179 (1971).

[12]On the other hand, the effect of electron-hole excitations on the deep density of states is mainly a broadening and softening of the individual plasmon satellite; in contrast to the effect of the excitation of electron-hole pairs on fast electrons, most of the change in spectral weight is at energies considerably smaller than the plasmon energy. Therefore this effect is mainly one of reshuffling the spectral weight within a plasmon satellite, without changing the relative weights of the satellites.

[13]D. C. Langreth, Phys. Rev. Lett. **26,** 1229 (1971).

[14]F. Brouers, Phys. Lett. **11,** 297 (1964); A. J. Glick and P. Longe, Phys. Rev. Lett. **15,** 589 (1965).

[15]L. Hedin, B. Lundqvist, and S. Lundqvist, in *Proceedings of the Third Materials Research Symposium on the Electron Density of States,* edited by L. H. Bennett, Natl. Bur. Std. Special Pub.No. 323, (U.S. GPO, Washington, D.C., 1971), p. 233.

[16]C. N. Berglund and W. E. Spicer, Phys. Rev. **136,** A1040 (1964).

[17]E. A. Stern and R. A. Ferrell, Phys. Rev. **120,** 130 (1960); R. H. Ritchie, Phys. Rev. **106,** 874 (1957).

[18]In our model this prediction becomes exact to the extent that $e^2/\hbar v \to 0$. The model, however, neglects certain effects (such as plasmon-plasmon interaction) which provide additional ways to reach a multiplasmon final state, thus strengthening the satellites over and above our model's predictions on the higher (number) density metals, these effects are expected to be small; a systematic method for calculating them is given in the last section of Ref. 10, but such calculations have not yet been done.

[19]Of the several relevant experimental papers [for example, Ref. 1 and Y. Baer and G. Busch, Phys. Rev. Lett. **30,** 280 (1973)], the only one we know of which quotes the strengths of the satellites is C. J. Vesely, D. L. Kingston, and D. W. Langer [Phys. Rev. (to be published)]. The results here are contradictory, but if the measured strength of the third satellite is disregarded because of the obvious experimental uncertainty, then their results would agree with our prediction. We might also mention that R. A. Pollak [Ph.D. thesis (University of California, Berkeley, 1972) (unpublished)] measures the $2S$ satellites in Al and finds a linearly decreasing strength ratio, apparently indicating that the intrinsic effect is weak.

[20]A word of warning, however: energy loss through a thin (or thick) film does not measure the same function.

[21]N. W. Ashcroft and W. L. Schaich, in Ref. 15.

[22]G. D. Mahan, Phys. Rev. B **2,** 4434 (1970).

[23]For example, D. C. Langreth, Phys. Rev. B **3,** 3120 (1971) (hereafter referred to as II).

[24]L. P. Kadanoff and G. Bajan, *Quantum Statistical Mechanics* (Benjamin, New York, 1962).

[25]V. Keldysh, Zh. Eksp. Teor. Fiz. **47,** 1515 (1964) [Sov. Phys.-JETP **20,** 1018 (1965)].

[26]Since the x-ray skin depth $\delta \gg l$, the inelastic mean free path of the photoelectron, our results will not be dependent on this assumption in the actual physical situation.

[27]This typifies our notation for the vectors. X is the x-component of the vector $\vec{X}$, and $\vec{X}_\parallel$ is the component of $\vec{X}$ in the plane parallel to the surface.

[28]We use the unit that $2m = \hbar = 1$ except for the $e^2/\hbar v$.

[29]M. Šunjić and A. A. Lucas, Phys. Rev. B **3,** 719 (1971).